Toxicology Research

Accepted Manuscript

ROYAL SOCIETY OF CHEMISTRY

www.rsc.org/toxicology

	Simunek, Tomas; Charles University in Prague, Faculty of Pharmacy in Hradec Kralove, Department of Biochemical Sciences

Synthesis and analysis of novel analogues of dexrazoxane and its open-ring hydrolysis product for protection against anthracycline cardiotoxicity *in vitro* and *in vivo*

Anna Jirkovská-Vávrová[a], Jaroslav Roh[a], Olga Lenčová-Popelová[b], Eduard Jirkovský[b], Kateřina Hrušková[a], Eliška Potůčková-Macková[a], Hana Jansová[a], Pavlína Hašková[a], Pavla Martinková[a], Tomáš Eisner[a], Marek Kratochvíl[a], Jan Šůs[a], Miloslav Macháček[a], Lucie Vostatková-Tichotová[a], Vladimír Geršl[b], Danuta S. Kalinowski[c], Mark T. Muller[d], Des R. Richardson[c], Kateřina Vávrová[a], Martin Štěrba[b], Tomáš Šimůnek[a,*]

[a]*Charles University in Prague, Faculty of Pharmacy in Hradec Králové, Heyrovského 1203, 500 05 Hradec Králové, Czech Republic*

[b]*Charles University in Prague, Faculty of Medicine in Hradec Králové, Šimkova 870, 500 38 Hradec Králové, Czech Republic*

[c]*Iron Metabolism and Chelation Program, Bosch Institute and Department of Pathology, University of Sydney, Sydney, Australia*

[d]*College of Medicine, Biomedical Research, University of Central Florida, 6900 Lake Nona Boulevard, Orlando, Florida 32827, U.S.A.*

***Corresponding author:**

Dr. Tomáš Šimůnek
Department of Biochemical Sciences
Charles University in Prague, Faculty of Pharmacy
Heyrovského 1203
500 05 Hradec Králové
Czech Republic
Tel.: +420 495 067 422
Fax: +420 495 067 168
E-mail: Tomas.Simunek@faf.cuni.cz

Abstract

Cardiotoxicity is a serious drawback of anthracycline anti-cancer drugs and dexrazoxane is the only cardioprotective agent with clinically established efficacy. Iron-mediated oxidative stress is traditionally believed to be the primary cause of anthracycline cardiotoxicity, and dexrazoxane-induced cardioprotection is attributed to iron chelating properties of its open ring metabolite, ADR-925, which may inhibit the oxidative injury. However, dexrazoxane is also a catalytic inhibitor of topoisomerase II (TOP2), and the role of oxidative stress in clinically relevant forms of cardiotoxicity has increasingly been questioned. In this study, novel analogues of dexrazoxane (MK-15, ES-5) and ADR-925 (KH-TA4, JR-159) were synthesized, and evaluated *in vitro* and *in vivo*. When examined in the leukemic cell line, HL-60, these novel analogues did not interfere with the anti-proliferative action of daunorubicin. In contrast to dexrazoxane, they had no anti-cancer effect on their own and the changes in the chemical structure resulted in a loss of TOP2 inhibitory activity. Although some of the novel compounds showed significant anti-oxidant and iron chelating properties *in vitro*, they did not protect isolated cardiomyocytes and rabbits from daunorubicin-induced cardiotoxicity and heart failure. Importantly, dexrazoxane has been found to be a relatively weak intracellular iron chelator and it failed to protect the isolated cardiomyocytes from model oxidative injury induced by hydrogen peroxide. However, in contrast to all novel analogues, dexrazoxane induced depletion of the TOP2 beta isoform. This isoform is typical for terminally differentiated cells and its genetic deletion has been reported to overcome anthracycline-induced cardiotoxicity. Hence, TOP2 beta, rather than (or along with) iron chelation, may be promising target for effective cardioprotection induced by bisdioxopiperazine agents.

Keywords: Anthracycline cardiotoxicity; Cardioprotection; Daunorubicin; Dexrazoxane (ICRF-187); Iron chelation; Topoisomerase II (TOP2).

Graphical Abstract

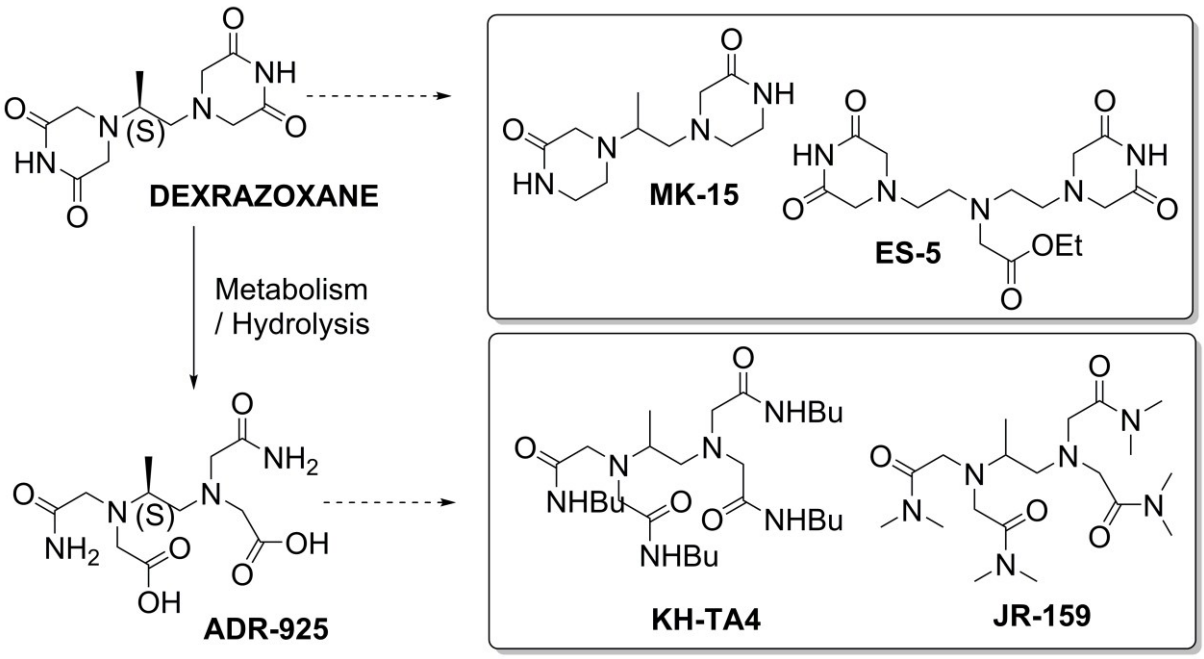

Abbreviations:

AcCN – acetonitrile; ANT – anthracycline; cTnT – cardiac troponin T; DAU – daunorubicin; DEX – dexrazoxane; DMEM – Dulbecco's Modified Eagle Medium; DMEM/F12 – DMEM with Ham's F-12 nutrient mixture (1:1); DMF – *N*,*N*-dimethylformamide; DMSO – dimethyl sulfoxide; DOX – doxorubicin; DTPA – diethylenetriaminepentaacetic acid; DTT – dithiothreitol; Et_2O – diethylether; EtOH – ethanol; FAC – ferric ammonium citrate; FBS – fetal bovine serum; FS – fractional shortening; GAPDH – glyceraldehyde 3-phosphate dehydrogenase; H_2O_2 – hydrogen peroxide; HEPES – 4-(2-hydroxyethyl)-1-piperazineethanesulfonic acid; HS – horse serum; LDH – lactate dehydrogenase; LV – left ventricular; MeOH – methanol; MTT – 3-(4,5-dimethylthiazol-2-yl)-2,5-diphenyltetrazolium bromide; NAD^+ – nicotinamide adenine dinucleotide; NVCMs – rat isolated neonatal ventricular cardiomyocytes; P/S – penicillin/streptomycin; PBS – phosphate-buffered saline; ppm – parts per million; PVDF – polyvinylidene fluoride; PYR – sodium pyruvate; RIPA – radioimmunoprecipitation assay; ROS – reactive oxygen species; SDS – sodium dodecyl sulphate; SIH – salicylaldehyde isonicotinoyl hydrazone; TEA – triethylamine; Tf – human transferrin; TOP2 – topoisomerase II; TOP2A – topoisomerase II alpha; TOP2B – topoisomerase II beta.

1 Introduction

Anthracyclines (ANTs), such as doxorubicin (DOX) or daunorubicin (DAU) are highly effective anti-neoplastic agents.[1] ANTs inhibit tumor growth mainly by blocking the function of topoisomerase IIα (TOP2A), an enzyme that is crucial for post-replicative decatenation and for alleviating super-helical torsion arising from DNA topology.[2] Although ANTs are more than 50 years old, they are still widely prescribed for the treatment of a number of hematological and solid malignancies.[3]

Clinically, ANTs are associated with a significant risk of cardiotoxicity.[1, 4-6] The most important are chronic forms of cardiotoxicity that develop months or years after the completion of chemotherapy and typically manifest as dilated cardiomyopathy and heart failure.[3] Despite numerous proposed theories, the exact pathophysiological mechanism(s) of ANT cardiotoxicity still remain(s) elusive. The dominant and most cited hypothesis implicates the iron (Fe)-mediated generation of reactive oxygen species (ROS).[7, 8] ANTs can induce the production of superoxide radicals *via* the quinone/semiquinone redox cycling of its aglycone.[9, 10] The superoxide dismutates into hydrogen peroxide (H_2O_2), which may in turn enter the Fe-catalyzed Haber-Weiss reaction, yielding hydroxyl radicals. The hydroxyl radical is an extremely reactive and toxic form of ROS that damage DNA, alter proteins and lipids and promote myocyte dysfunction and death.[11] Furthermore, ANTs are able to form complexes with free Fe ions and undergo a cascade of reactions resulting in further hydroxyl radical production.[7]

To date, the only pharmacological agent with the demonstrated ability to prevent ANT-induced cardiotoxicity is dexrazoxane (DEX, ICRF-187, (*S*)-4-[2-(3,5-dioxopiperazin-1-yl)propyl]piperazine-2,6-dione; Fig. 1).[12] According to the prevailing hypothesis, DEX protects cardiomyocytes against ANT-induced damage *via* its metal-chelating hydrolysis product, ADR-925 (Fig. 1), an analogue of the well-known metal chelator EDTA.[13, 14] ADR-925 may act by displacing Fe from Fe-ANT complexes and/or by chelating free redox-active intracellular Fe ions, and thus, prevent site-specific Fe-based ROS damage.[15, 16] Of note, DEX has also been shown protective against a variety of other toxicities (apart from ANT-induced cardiotoxicity) associated with oxidative stress. [17, 18] However, DEX is also a powerful catalytic TOP2 inhibitor[19] and a recent study suggested that the beta-isoform of this enzyme is the key molecular target mediating the cardiotoxicity.[20] Furthermore, DEX has been found to deplete topoisomerase IIβ (TOP2B) in H9c2 myoblasts by a yet-undisclosed mechanism(s), and this effect might be associated with its cardioprotective activity.[21]

Randomized clinical trials have clearly demonstrated that administration of DEX together with ANTs significantly reduces incidence of cardiac events and permits the administration of higher cumulative doses of ANTs.[22, 23] On the other hand, DEX therapy is also associated with certain disadvantages. For example, DEX aggravates ANT-induced hematotoxicity, particularly leucopenia.[16, 24] DEX has also been associated with a higher incidence of secondary malignancies,[25] as well as interference with ANT anti-tumor efficacy.[26] Although these findings are controversial, they have already had a significant impact on the recommendations[27] for the clinical application of DEX. Hence, despite the unequivocal ability of DEX to prevent ANT-induced cardiotoxicity in adults and children, either real or perceived problems attributed to DEX have resulted in a reduction in use in the clinical oncology community at large. However, the remarkable cardioprotective potential of DEX has strongly

encouraged the search for safer DEX alternatives and analogues with retained powerful cardioprotective effects. Most *in vitro* and *in vivo* studies of alternative cardioprotectives focused so far on various antioxidants, flavonoids or iron chelators, with promising results from high-dose and acute settings, which were not affirmed in clinically relevant chronic models.[28] Surprisingly, only a few DEX and/or ADR-925 derivatives or analogues have been studied so far, which contributes to the very limited insight into the structure-activity relationships of these agents. Furthermore, the uncertainty about the specific pharmacological effect of DEX responsible for its cardioprotective action generally hinders the development of novel and effective cardioprotective strategies.

The aims of this study were to synthesize novel analogues of DEX and its putative active metabolite ADR-925 (Fig. 1) and to evaluate their cardioprotective potential both *in vitro* and *in vivo*. To this end, we used primary cultures of rat isolated neonatal ventricular cardiomyocytes (NVCMs) and a well-established model of chronic ANT-induced heart failure in rabbits.[29-31] The Fe chelation and mobilization properties of the examined agents as well as their effects on TOP2 activity and protein levels were used to assess the properties necessary for effective cardioprotection.

2 Materials and methods

2.1 Materials

Dulbecco's Modified Eagle Medium (DMEM), DMEM with Ham's F-12 nutrient mixture (DMEM/F12), horse serum (HS), fetal bovine serum (FBS), penicillin/streptomycin solution (5000 U/mL; P/S) and sodium pyruvate solution (100 mM; PYR) were purchased from Lonza (Basel, Switzerland). The sera were heat-inactivated prior to use. DEX was obtained from Huaren Chemicals (Changzhou, Jiangsu, China) and the identity and purity of the compound was also verified in-house using appropriate methods described below. RPMI-1640 medium with L-glutamine and $NaHCO_3$, pyruvate-free DMEM, lactic acid, nicotinamide adenine dinucleotide (NAD^+), MTT (3-(4,5-dimethylthiazol-2-yl)-2,5-diphenyltetrazolium bromide), as well as other chemicals (*e.g.*, the constituents of various buffers) were purchased from Sigma-Aldrich (St. Louis, Montana, U.S.A.) or Penta (Prague, Czech Republic), and were of the highest available pharmaceutical or analytical grade. Dimethyl sulfoxide (DMSO) was used to dissolve the examined compounds.

2.2 Synthesis of dexrazoxane and ADR-925 analogues

All chemicals for synthesis were obtained from Sigma-Aldrich (St. Louis, Montana, U.S.A.) and used as received. Thin-layer chromatography was performed on Merck aluminum sheets with silica gel 60 F254 or Merck aluminum sheets with silica gel 60 RP-18 F254s (Merck KGaA, Darmstadt, Germany). Merck Kieselgel 60 (0.040-0.063 mm) was used for column chromatography. The melting points of the compounds were recorded on a Büchi B-545 apparatus, and are uncorrected. Infrared spectra were measured on Nicolet 6700 (ATR mode) (Thermo Fisher Scientific, Waltham, Massachusetts, U.S.A.). ^1H and ^{13}C NMR spectra were

recorded using a Varian Mercury Vx BB 300 or VNMR S500 NMR spectrometer (Agilent Technologies, Santa Clara, California, U.S.A). Chemical shifts were reported as δ values in parts per million (ppm), and were indirectly referenced to tetramethylsilane *via* the solvent signal. Elemental analysis was carried out using an EA1110CE Automatic Microanalyzer (Fisons Instruments, Milan, Italy). Mass spectra were recorded using an Agilent 500 Ion Trap LC/MS (Agilent Technologies, Santa Clara, California, U.S.A.).

2.2.1 *Synthesis of Ethyl-2-{bis[2-(3,5-dioxopiperazin-1-yl)ethyl]amino}acetate (ES-5; Fig. 2)*

2-{Bis[2-(3,5-dioxopiperazin-1-yl)ethyl]amino}acetic acid: A suspension of diethylenetriaminepentaacetic acid (10 g, 25.4 mmol) in formamide (40 mL) was stirred and heated under a vacuum (1.5-2 kPa) for 1 h. The reaction flask was then filled with argon, and the reaction was heated to 150-160 °C/5 h under an argon atmosphere. Approximately 30 mL of formamide was evaporated under reduced pressure and the dark residue was cooled to room temperature, diluted with 20 mL of methanol and cooled until a precipitate formed. The product was filtered, washed several times with methanol and dried.

Yield: 68% (6.14 g) as a cream-colored solid; mp 254 °C; ^{1}H NMR (500 MHz, DMSO-d_6) δ 11.06 (s, 2H), 3.34 (s, 8H), 3.31 (s, 2H), 2.78 (t, J = 6.4 Hz, 4H), 2.55 (t, J = 6.4 Hz, 4H); ^{1}H NMR (300 MHz, D_2O) δ 3.82 (s, 2H), 3.56 (s, 8H), 3.50-3.41 (m, 4H), 3.04-2.94 (m, 4H); ^{13}C NMR (126 MHz, DMSO-d_6) δ 171.76, 171.55, 55.31, 55.24, 52.56, 50.90; ^{13}C NMR (75 MHz, D_2O) δ 173.45, 170.56, 57.20, 54.83, 51.80, 49.30. LRMS *m/z* (APCI) 356.6 (100, $M+H^+$), 357.6 (16%).

Ethyl-2-{bis[2-(3,5-dioxopiperazin-1-yl)ethyl]amino}acetate: Amino acid (2 g, 5.63 mmol) and K_2CO_3 (0.39 g, 2.82 mmol) were suspended in DMSO under vigorous stirring. Ethylbromide (0.4 mL, 5.35 mmol) was added dropwise, and the reaction mixture was stirred at room temperature for 10 h. The reaction mixture was filtered, the DMSO was evaporated under reduced pressure, and the residue was purified using column chromatography on silica (mobile phase: ethyl acetate) and subsequently recrystallized (acetone/ethyl acetate).

Yield: 56% (1.2 g) as a yellowish solid; mp 110 °C; R_f (ethyl acetate) 0.18; ^{1}H NMR (300 MHz, DMSO-d_6) δ 11.06 (s, 2H), 4.02 (q, J = 7.1 Hz, 2H), 3.38 (s, 2H), 3.32 (s, 8H), 2.69 (t, J = 6.3 Hz, 4H), 2.56-2.46 (m, 4H), 1.16 (t, J = 7.1 Hz, 3H); ^{13}C NMR (75 MHz, DMSO) δ 171.66, 171.27, 59.85, 55.41, 54.60, 53.27, 50.83, 14.31. LRMS *m/z* (APCI) 384.3 (100, M+H$^+$), 385.1 (18%).

2.2.2 *Synthesis of 4,4'-(Propane-1,2-diyl)bis(piperazin-2-one) (MK-15; Fig. 2)*

Piperazin-2-one: Ethyl bromoacetate (27.5 mL, 0.25 mol) was added in several portions to a stirring suspension of ethylenediamine (160 mL, 2.4 mol) and K_2CO_3 (36 g, 0.26 mol) in acetonitrile (AcCN) (1 L). The reaction mixture was heated to reflux for 6 h under microwave irradiation. The reaction mixture was then cooled to room temperature, filtered, and the volatiles were evaporated under reduced pressure. The residue was recrystallized twice from acetone.

Yield: 65% (16 g) as a yellowish crystalline solid; mp 133 °C; ^{1}H NMR (300 MHz, D_2O) δ 3.40 (s, 2H), 3.38-3.28 (m, 2H), 3.00-2.89 (m, 2H). ^{13}C NMR (75 MHz, D_2O) δ 173.21, 47.88, 41.99, 40.93.

4,4'-(Propane-1,2-diyl)bis(piperazin-2-one): Piperazin-2-one (14.95 g, 0.149 mol), K_2CO_3 (20.6 g, 0.149 mol) and 1,2-dibromopropane (7.8 mL, 0.074 mol) were heated under an argon atmosphere to 90 °C for 10 h in 100 mL of *N*,*N*-dimethylformamide (DMF). The reaction mixture was cooled and filtered, and the DMF was evaporated under reduced pressure. The residue was purified using silica gel column chromatography (mobile phase: $CHCl_3$/MeOH, 5:1)

Yield: 26% (4.66 g) as a yellowish crystalline solid; mp 155-156 °C (with decomp.); R_f ($CHCl_3$/MeOH, 2:1) 0.42; ^{1}H NMR (300 MHz, D_2O) δ 3.42-3.32 (m, 4H), 3.31 (s, 2H), 3.23 (s, 2H), 3.08 – 2.94 (m, 1H), 2.93-2.81 (m, 3H), 2.80-2.63 (m, 2H), 2.57-2.46 (m, 1H), 1.11 (d, J = 6.5 Hz, 3H); ^{1}H NMR (300 MHz, DMSO-d_6) δ 7.69 (s, 1H), 7.65 (s, 1H), 3.16-3.02 (m, 6H), 2.95-2.90 (m, 2H), 2.91-2.80 (m, 1H), 2.66-2.39 (m, 5H), 2.22 (dd, J = 12.5, 7.1 Hz, 1H), 0.91 (d, J = 6.5 Hz, 3H); ^{13}C NMR (75 MHz, D_2O) δ 172.51, 171.98, 59.69, 56.18, 55.33, 51.83, 48.55, 44.05, 40.99, 40.44, 13.15. ^{13}C NMR (75 MHz, DMSO-d_6) δ 168.53, 168.02, 59.90, 57.42, 54.54, 52.82, 49.36, 44.75, 41.06, 40.60, 13.05; LRMS *m/z* (APCI) 241.4 (100, $M+H^+$), 242.2 (12%).

2.2.3 *Synthesis of N,N,N',N'-tetrakis(N,N-dimethylcarbamoylmethyl)-1,2-diaminopropane (JR-159; Fig. 2)*

A mixture of 1,2-diaminopropane (1 mL, 11.7 mmol), 2-chloro-*N*,*N*-dimethylacetamide (7.24 mL, 70.4 mmol), K_2CO_3 (10 g, 72.4 mmol) and NaI (1 g, 6.67 mmol) in AcCN (60 mL) was stirred and heated to reflux for 4 h under microwave irradiation. The reaction mixture was cooled and stirred overnight at room temperature. The suspension was then filtered, and the AcCN was evaporated under reduced pressure. The residue (9 g) was purified by column chromatograph after three consecutive runs (1. mobile phase: Acetone/TEA), gradient 15:1-10:1; 2. mobile phase: Acetone/EtOH/TEA, gradient 10:0:1-10:10:1, 3. mobile phase: EtOH/TEA, gradient 10:0-10:1).

Yield: 21% (1.04 g) as a yellowish viscous oil; R_f (EtOH) 0.1; ^{1}H NMR (300 MHz, DMSO-d_6) δ 3.48-3.34 (m, 6H), 3.24-3.10 (m, 2H), 3.03 (s, 6H), 2.95 (s, 6H), 2.86-2.68 (m, 14H), 2.38 (dd, J = 12.4, 6.1 Hz, 1H), 0.88 (d, J = 6.0 Hz, 3H). ^{13}C NMR (75 MHz, DMSO-d_6) δ 170.12, 169.99, 56.89, 55.96, 53.82, 52.72, 36.61, 36.41, 35.19, 34.99, 13.21. LRMS *m/z* (APCI) 415.5 (100, M+H$^+$), 416.5 (21%).

2.2.4 *Synthesis of N,N,N',N'-tetrakis(N-butylcarbamoylmethyl)-1,2-diaminopropane (KH-TA4; Fig. 2)*

***N*-Butyl-2-bromoacetamide:** A solution of bromoacetylbromide (2.08 g, 0.01 mol) in dry Et_2O (6 mL) was cooled to -20 °C. A solution of butylamine (1.51 g, 0.02 mol) in 6 mL of dry Et_2O was added dropwise over the course of 30 min. The reaction mixture was stirred at -20 °C for 30 min, after which 12 mL of cold water was added to the reaction mixture. The

organic layer was removed and washed twice with 12 mL of 1 M HCl, 12 mL of 1 M NaOH and 12 mL of brine. The organic layer was dried with anhydrous Na_2SO_4 and evaporated under reduced pressure.

Yield: 65% (1.26 g) as a colorless oil, solidifying at 4 °C to an amorphous solid. ^{1}H NMR (300 MHz, DMSO-d_6) δ 8.22 (s, 1H), 3.80 (s, 2H), 3.09-3.01 (m, 2H), 1.46-1.17 (m, 4H), 0.86 (t, J = 7.2 Hz, 3H); ^{13}C NMR (126 MHz, DMSO-d_6) δ 165.99, 38.81, 31.07, 29.77, 19.63, 13.79.

***N,N,N′,N′*-tetrakis(*N*-butylcarbamoylmethyl)-1,2-diaminopropane:** 1,2-diaminopropane (0.28 g, 0.004 mol) was dissolved in 10 mL of AcCN. Potassium carbonate (2.6 g, 0.019 mol) and *N*-butyl-2-bromoacetamide (3.7 g, 0.019 mol) were added, and the reaction mixture was heated in a microwave reactor to reflux for 4 h. The reaction mixture was cooled to 4 °C overnight. The resulting solid was filtered off, washed thoroughly with water and dried under reduced pressure.

Yield: 88% (1.85 g) as a white solid, mp 160-162 °C. ^{1}H NMR (500 MHz, $CDCl_3$) δ 7.58 (t, J = 5.8 Hz, 2H), 7.49 (t, J = 5.9 Hz, 2H), 3.34-3.02 (m, 16H), 2.96-2.87 (m, 1H), 2.58 (dd, J = 13.8, 9.8 Hz, 1H), 2.37 (dd, J = 13.8, 4.6 Hz, 1H), 1.54-1.41 (m, 8H), 1.38-1.26 (m, 8H), 0.94-0.87 (m, 15H). ^{13}C NMR (126 MHz, $CDCl_3$) δ 170.97, 170.36, 58.98, 58.90, 55.21, 55.00, 39.22, 39.10, 31.66, 31.64, 20.11, 13.71, 13.70, 12.30. LRMS *m/z* (APCI) 527.5 (100, $M+H^+$), 528.5 (29%).

2.3 Cell culture, *in vitro* toxicity and proliferation assessments

The HL-60 acute promyelocytic leukemia cell line,[32] was purchased from the American Type Culture Collection (Manassas, Virginia, U.S.A.) and cultured in RPMI-1640 supplemented with 10% FBS, 1% P/S in 75 cm^2 tissue culture flasks at 37 °C in a humidified atmosphere with 5% CO_2. For cytotoxicity assays, the cells were plated in 96-well plates in a density of 10,000 cells/well. The cells were incubated with the indicated agents for 72 h/37 °C. The proliferation was determined using MTT assays. Briefly, 25 µL of a 3 mg/mL MTT solution in PBS was added to each well, and after 2 h of incubation at 37 °C the cells were lysed with lysis buffer (isopropanol, 0.1 M HCl, 5% Triton X-100) for 30 min at room temperature. After the formazan was dissolved, the absorbance of the samples was measured at 570 and 690 nm.

NVCMs were isolated from 1-3 day old Wistar rats using standard methods.[33-35] The use of animals was approved by the Charles University Faculty of Pharmacy Animal Care Committee. The neonatal hearts were minced in ADS buffer (1.2 mM $MgSO_4.7H_2O$; 116 mM NaCl; 5.3 mM KCl; 1.13 mM $NaH_2PO_4.H_2O$; 20 mM HEPES) on ice and serially digested at 37 °C with collagenase type II (Invitrogen, Carlsbad, California, U.S.A.). The cell suspension was pre-plated on a 150-mm Petri dishes (suspension from approximately 20 hearts/dish) for 2 h at 37 °C to minimize contamination with fibroblasts. The NVCM cells were then plated on 12-well gelatin-coated plates at 80,000 cells/well. NVCMs were cultured at 37 °C in a 5% CO_2 atmosphere in DMEM/F12 medium supplemented with 10% HS, 5% FBS, 4% PYR and 1% P/S. Newly isolated NVCMs were left for 40 h to attach properly and allowed form a culture of spontaneously beating cardiomyocytes, and then the medium changed to DMEM/F12 supplemented with 5% FBS, 4% PYR and 1% P/S.

For experiments, the medium was changed to serum- and pyruvate-free DMEM/F12 with 1% P/S. The myocytes were pre-treated with DEX, or the novel analogues for 0, 3, 6 or 24 h/37 °C and then co-incubated with 1.2 μM DAU for 3 h/37 °C. After these incubations, the culture medium was changed and the cells were post-incubated with DEX or the novel analogues for 48 h/37 °C. Alternatively, after pre-treatment, the cells were co-incubated with 300 μM H_2O_2 for 48 h. A sample of the culture medium was taken from each well to assess lactate dehydrogenase (LDH) activity as an indice of membrane damage.[36-38] The control wells were treated with lysis buffer (0.1 M potassium phosphate, 1% Triton X-100, 1 mM DTT, 2 mM EDTA, pH 7.8, 15 min/room temperature) to measure the total cellular LDH level. The samples were frozen immediately and stored at -80 °C until they were analyzed. The activity of LDH was assayed in Tris-HCl buffer (pH 8.9) containing 35 mM lactic acid and 5 mM NAD^+. The rate of NAD^+ reduction was monitored spectrophotometrically at 340 nm for 2 min/37 °C. The slope of the linear region was calculated, and the data were expressed as a percent of total LDH.

Changes in cellular morphology were assessed using an Eclipse TS100 inverted epifluorescence microscope (Nikon Corporation, Tokyo, Japan) and NIS-Elements AR 2.20 software (Laboratory Imaging s.r.o., Prague, Czech Republic). To visualize active mitochondria, NVCMs were loaded with 0.5 μM JC-1 (Molecular Probes/ Thermo Fisher Scientific, Inc., Waltham, Massachusetts, U.S.A.) for 30 min/37 °C after the 3-h pre-treatment/37 °C with the novel analogues (30 μM) and subsequent incubation with 1.2 μM DAU for 3 h/37 °C with a 48-h drug-free period. At low concentrations, JC-1 exists within cells in a green-fluorescent monomeric form and accumulates in actively respiring mitochondria with membrane potential difference ($\Delta\Psi_m$) between the inner and outer

mitochondrial membrane. This $\Delta\Psi_m$-dependent formation of "J-aggregates" is represented by a shift from green to red fluorescence.

The H9c2 cell line, derived from embryonic rat heart tissue,[39] was purchased from the American Type Culture Collection (Manassas, Virginia, U.S.A.) and were cultured in DMEM supplemented with 10% FBS, 1% P/S and 10 mM HEPES in 75 cm^2 tissue culture flasks at 37 °C in a humidified atmosphere of 5% CO_2. Sub-confluent cells were passaged every 3-4 days. In the calcein assay, cells were seeded in 12-well plates (75,000 cells/well), allowed to attach for 24 h and then the culture medium was replaced with serum- and pyruvate-free DMEM. In the serum free media, the cells were essentially non-proliferating and were used for experiments.

2.4 *In vivo* cardiotoxicity and cardioprotection studies

To examine the *in vivo* cardioprotective effects of the novel DEX analogues in a pilot study, a well-established model of chronic ANT cardiotoxicity in rabbits was used,[29, 30, 40] Chinchilla male rabbits (~3.5 kg; $n = 34$) were randomized into several groups. Cardiotoxicity was induced with DAU (3 mg/kg, *i.v.*, Pfizer Inc., New York, New York, U.S.A, $n = 6$), while a control group received saline (1 mL/kg, *i.v.*, $n = 6$). All procedures using these animals were approved by the Charles University Faculty of Medicine Animal Care Committee. Dexrazoxane (60 mg/kg, Cardioxane, Novartis, Basel, Switzerland, $n = 6$), MK-15 (60 mg/kg, $n = 5$), ES-5 (60 mg/kg, $n = 3$), KH-TA4 (25 mg/kg, $n = 7$) and JR-159 (50 mg/kg, $n = 1$) were dissolved in saline and administered intraperitoneally 30 min prior to each DAU administration. All of the drugs were administered once weekly for 10 weeks, which is a

standard procedure used previously for chronic DAU-induced cardiotoxicity development in rabbits.[30] DEX was administered at the recommended 1:20 dose ratio to DAU that has been previously demonstrated to be effective and well-tolerated in rabbits.[30, 31] The tolerability of the repeated weekly co-administration of the newly synthesized agents and DAU was estimated prior to the analysis of potential cardioprotective effects. The results of these preliminary experiments performed with 60 mg/kg of the drugs and the same schedule as describe above suggested a necessary dose reduction of KH-TA4 and JR-159 to 25 and 50 mg/kg, respectively.

The administration of drugs, blood sampling and non-invasive measurements of cardiac function were carried out under combined light anesthesia of ketamine (30 mg/kg, i.m.) and midazolam (1.25 mg/kg, i.m.). Weight gain was monitored weekly, and changes in behavior and possible external signs of toxicity were observed daily. The study was terminated 5-7 days after the last drug administration by pentobarbital overdose. During autopsy or necropsy, gross pathological changes of the heart, as well as the presence of pleural effusions and ascites were evaluated.

The left ventricular (LV) systolic function was analyzed by echocardiography (Vivid 4, 10 MHz probe; GE Healthcare, Buckingham, U.K.). The LV fractional shortening (FS), an index of the LV systolic function, was obtained from LV end-systolic and end-diastolic diameters as determined by guided M-mode scanning from the left parasternal long and short axis view.[41] The examination was performed at the beginning of the study and weekly during the later stages of the study (8^{th}-11^{th} week), when the DAU-induced decline in systolic function is observed.[30]

The concentration of cardiac troponin T (cTnT) in plasma was determined using an Elecsys Tropo T hs (Roche Diagnostics/Hoffman-La Roche Ltd., Basel, Switzerland) at the beginning of the study, and before the 5th, 8th and 10th administration of the drug and at the end of the study.

2.5 Determination of Fe-chelating properties

The experiments analyzing the Fe-chelating efficacy of the compounds in cultured cells were performed according to Glickstein *et al.*[42] with slight modifications. H9c2 cells were seeded in 96-well plates (10,000 cells/well) and loaded with 100 μM ferric ammonium citrate (FAC) in serum-free medium for 24 h. The cells were then washed, and to prevent potential interferences from trace contaminants, the medium was replaced with a buffer prepared from Millipore-filtered (demineralized) water, containing 116 mM NaCl, 5.3 mM KCl, 1 mM $CaCl_2$, 1.2 mM $MgSO_4$, 1.13 mM NaH_2PO_4, 5 mM glucose and 20 mM HEPES (pH 7.4). The cells were then loaded for 30 min at 37 °C with 1 μM of the cell-permeable acetoxymethyl ester of calcein green (Molecular Probes/ Thermo Fisher Scientific, Inc., Waltham, Massachusetts, U.S.A.) and then washed with calcein-free buffer. Cellular esterases cleave the acetoxymethyl groups to form the membrane-impermeable calcein green, and this fluorescence can be quenched by FAC. Intracellular fluorescence (λ_{ex} = 488 nm; λ_{em} = 530 nm) was then followed over time (1 min before and 10 min after the addition of chelator) at 37 °C using an Infinite 200 M plate reader (Tecan Austria GmbH, Grödig, Austria). The novel agents were compared to a previously characterized [33] chelator (salicylaldehyde isonicotinoyl hydrazone, SIH), used a positive control.

2.6 Effect of the agents on ^{59}Fe mobilization from cells

For ^{59}Fe mobilization studies, H9c2 cells were seeded in 35 mm Petri dishes (250,000 cells/dish). Human transferrin (Tf) was labeled with ^{59}Fe (DuPont NEN, Boston, Massachusetts, U.S.A.) to produce $^{59}Fe_2$-Tf using established methods.[43, 44] Unbound ^{59}Fe was removed by exhaustive vacuum dialysis against a large excess of 0.15 M NaCl buffered to pH 7.4 with 1.4% $NaHCO_3$.[43, 44]

To examine the ability of the novel agents to mobilize ^{59}Fe from H9c2 cells, Fe efflux experiments were performed using established techniques.[43, 45] Briefly, after pre-labeling the cells with ^{59}Fe-Tf (0.75 μM) for 3 h/37 °C, the cells were washed four times with ice-cold PBS and subsequently incubated with the novel agents (25 μM) for 3 h/37 ºC. The culture medium containing the released ^{59}Fe was then separated from the cells. Radioactivity was measured in both the cell pellet and supernatant using a γ-scintillation counter (Wallac Wizard 3, Turku, Finland). The novel agents were compared to the reference chelator, SIH, which was used as a positive control as it is known to markedly increase cellular ^{59}Fe release.[46]

2.7 Fe displacement from the DAU-Fe complex

The rate of Fe displacement from the DAU-Fe complex by the studied substances was measured using spectrophotometric assays as described before.[47, 48] Briefly, a complex of DAU and Fe was prepared by adding $FeCl_3$ in 15 mM HCl to a DAU solution. The resulting complex (3:1), which revealed a typical absorption band at λ = 600 nm was added to reaction buffer (50 mM Tris/150 mM KCl, pH = 7.4, room temperature) in a glass cuvette to yield a final concentration of 45 μM DAU and 15 μM Fe^{3+}. After 4 min of equilibration, the novel

analogues (or the reference Fe chelator, SIH) were added to obtain a final concentration of 100 μM. The absorbance of the reaction at λ = 600 nm was then measured for 4 min at room temperature using a spectrophotometer (Heliosβ, Spectronic Unicam, Cambridge, U.K.).

2.8 Topoisomerase IIα (TOP2A) activity assay

TOP2A inhibition assays were performed using the Topoisomerase II Drug Screening Kit (TopoGEN Inc., Port Orange, Florida, U.S.A.) according to the manufacturer's instructions. Briefly, 200 ng of pHOT1 supercoiled DNA was incubated with 1 unit of TOP2A in a reaction buffer containing 0.1 M Tris-HCl, 0.3 M NaCl, 20 mM $MgCl_2$, 1 mM DTT, 60 μg/mL bovine serum albumin and 100 μM of each compound for 30 min/37 °C. The reaction was then stopped by using an incubation of the reaction mixture with 1% SDS and 50 ng of proteinase K (15 min/37 °C). Gel loading buffer (1/10 volume; 0.25% bromphenol blue and 50% glycerol) was added, and the samples were analyzed on a 1% agarose gel according to the commercial supplier. Electrophoresis was conducted at 10 V/cm for approximately 1 h. Gels were stained with ethidium bromide (0.5 μg/mL) for 15 min and destained in water for 10 min prior to visualizing DNA bands using a GelDoc with Quantity One software (Bio-Rad, Hercules, California, U.S.A.).

2.9 Western blot analysis of topoisomerase IIβ (TOP2B) in cardiomyocytes

The NVCMs were plated onto 60 mm Petri dishes and incubated with DEX, MK-15, ES-5, KH-TA4 or JR-159 for 3, 6, 12 or 24 h/37 °C, washed twice with ice-cold PBS, harvested with a cell scraper and centrifuged at 700 × *g*/10 min/4 °C. The supernatant was discarded, and the cell pellets were kept at -80 °C until homogenization in RIPA buffer with phosphatase

and protease inhibitor solution (Thermo Fisher Scientific Inc., Waltham, Massachusetts, U.S.A. and Roche, Basel, Switzerland, respectively) with brief vortexing, sonication on ice (90 s, 1 cycle, 100% amplitude; Ultrasonic Processor UP100H, Hielscher, Germany) and shaking (700 rpm, 1°C, 30 min; ThermoMixer C, Eppendorf AG, Hamburg, Germany). After centrifugation (16,000 × g, 1°C, 15 min), the supernatant was collected and 10 µg of protein was loaded into each lane of a Mini-PROTEAN Any kD TGX Precast Gel (Bio-Rad, Hercules, California, U.S.A.). After separation, the proteins were transferred onto a PVDF membrane (Pall Corporation, Port Washington, New York, U.S.A.) using a Trans-Blot SD Semi-Dry Electrophoretic Transfer Cell (Bio-Rad, Hercules, California, U.S.A.). Rabbit monoclonal anti-TOP2B (Abcam, Cambridge, U.K.; dilution 1:7,500) was used as a primary antibody and horseradish peroxidase-conjugated donkey anti-rabbit IgG (GE Healthcare, Wilmington, Massachusetts, U.S.A.; dilution 1:15,000) was used as the secondary antibody. The BM Chemiluminescence Blotting Substrate (Roche, Basel, Switzerland) was used for detection. Densitometric quantification was performed using Quantity One software (Bio-Rad, Hercules, California, U.S.A.). Protein loading was evaluated using an anti-GAPDH antibody (Sigma-Aldrich St. Louis, Montana, U.S.A.; dilution 1:2,000) and a horseradish peroxidase-conjugated goat anti-mouse IgG (DakoCytomation/ Dako Denmark A/S, Glostrup, Denmark; dilution 1:10,000).

2.10 Statistical analysis

The data are presented as mean ± SD and were subjected to one-way ANOVA with Holm-Sidak's post-hoc test. Data without normal distribution are presented as median ± interquartile range and were subjected to ANOVA on Ranks with Dunn's post-hoc test. Data were processed using GraphPad Prism 6.00 for Windows (GraphPad Software, Inc., La Jolla,

California, U.S.A.). All measurements were performed in more than three independent experiments. In the case of the TOP2A activity assays, a representative measurement from three independent measurements is presented.

3 Results

3.1 Syntheses of novel analogues of DEX and ADR-925

A major aim of this investigation was to synthesize novel analogues of DEX and its putative active metabolite, ADR-925 (Fig. 1), and to evaluate their cardioprotective potential both *in vitro* and *in vivo*. The current study resulted in the synthesis of two previously undescribed DEX analogues, namely ES-5 and MK-15, and two new ADR-925 analogues, JR-159 and KH-TA4. Investigation of their activity was important for understanding the structure-activity relationships of this group of agents, which may lead to compounds with even greater efficacy than DEX in terms of their ability to prevent ANT-mediated cardiotoxicity.

For the synthesis of MK-15, piperazin-2-one was prepared first from the reaction of ethyl 2-bromoacetate with ethylenediamine in acetonitrile (Fig. 2A). We improved the previously described reaction protocol,[49-51] and this enabled us to obtain a sufficient amount of pure piperazin-2-one by simple work-up and final recrystallization from acetone. The reaction of piperazin-2-one with 1,2-dibromopropane in DMF led to the formation of MK-15, which was purified by column chromatography (Fig. 2A).

The chemical synthesis of ES-5 was based on the cyclization of the terminal carboxylic acids of diethylenetriaminepentaacetic acid (DTPA) in formamide (Fig. 2B). In contrast to previously published observations,[52] the central carboxyl remained unmodified and the amino acid with terminal piperazin-2,6-dione rings was isolated. This compound was found to be soluble in water and partially soluble in DMSO. The target ethyl ester, ES-5, was obtained in

sufficient amount by the alkylation of the carboxylate in DMSO (Fig. 2B). This was accompanied by the formation of *N*-alkylation side-products on the imide nitrogens, which had to be carefully separated using column chromatography.

Both of the ADR-925 analogues (JR-159 and KH-TA4) were prepared from the reaction of 1,2-diaminopropane with the corresponding *N*-substituted 2-haloacetamide in acetonitrile (Fig. 2C,D). These procedures led to the formation of a mixture of products, especially tri- and tetra-substituted 1,2-diaminopropane and also quaternary ammonium salts. In the case of KH-TA4, the product crystallized from the reaction mixture, simple filtration and washing with water yielded the pure product. The purification of JR-159 was more complicated, as the product and by-products were viscous liquids that are highly soluble in water and also polar organic solvents with nearly identical retention on silica gel and C-18 reverse phase. Therefore, multiple consecutive column chromatography steps were necessary to obtain pure JR-159.

3.2 *In vitro* toxicity and proliferation assessments

3.2.1 *Proliferation of HL-60 cell line*

The anti-proliferative activity of the newly synthesized analogues of DEX (MK-15 and ES-5) and ADR-925 (KH-TA4 and JR-159) were first examined using a 72 h incubation with the human acute promyelocytic leukemia HL-60 cell line (Fig. 3). When assayed as single agents, only DEX (IC_{50} = 25 μM; Fig. 3A) and KH-TA4 (IC_{50} = 39 μM; Fig. 3D) demonstrated sufficient anti-proliferative effects to achieve an IC_{50} value within the concentration range

assessed (≤100 μM). The other analogues did not show anti-proliferative effects in the concentration range assessed, and thus, IC_{50} values for these compounds were not achieved.

Experiments were then undertaken to assess the effects of DEX and the novel analogues on the anti-proliferative activity of DAU (Fig. 3). The novel agents, when assayed at 10 μM and the maximal achievable concentration (100 μM), did not compromise the anti-proliferative activity of 15 nM DAU (*i.e.,* a concentration that corresponds to its IC_{50} value). In contrast, all the studied compounds increased the anti-proliferative effects of DAU in leukemic cells at both tested concentrations (Fig. 3).

3.2.2 *Toxicity to neonatal ventricular rat cardiomyocytes*

The toxicity of DEX and the novel analogues was then assessed using isolated NVCMs after a 48 h incubation. LDH release was used as a marker of plasma membrane damage and cytotoxicity. As seen in Fig. 4A, the analogues were generally non-toxic at the concentrations tested (≤100 μM), with exception of KH-TA4, which showed rather minor, but statistically significant ($p \leq 0.01$) toxicity in NVCMs. In fact, approximately 13% of total cellular LDH (compared to ~10% in control cells) was released upon incubation with KH-TA4 at its highest concentration (100 μM; Fig. 4A).

3.2.3 *Protection of cardiomyocytes from the toxicity of DAU or H_2O_2*

The novel DEX analogues were then thoroughly examined for their potential to protect NVCMs from the toxicity mediated by exposure to 1.2 μM DAU (Fig. 4B). In addition to

dose-dependence, pre-incubation of the cells with the potential cardio-protective agents for varying incubation times before DAU treatment was also examined. The exposure of cardiomyocytes to DAU induced significant ($p \leq 0.0001$) LDH release (~50% of total cellular LDH as compared to ~10% in the control cells). DEX was able to mediate significant ($p \leq 0.0001 - 0.05$) protection of cardiomyocytes against DAU at all concentrations assessed (10, 30, 100 μM) and pre-incubation times (Fig. 4B).

Of the novel agents, only ES-5 showed marked protection against DAU-induced toxicity comparable to DEX only when the lowest concentrations of ES-5 were used upon 0-6 h pre-incubation. However, when longer pre-incubation times (24 h) or higher concentrations were employed, the protective effect was lost. Of the other compounds, MK-15 demonstrated a slight, but not significant, decrease in LDH release in the absence of pre-incubation. The analogues of ADR-925 were essentially not protective against DAU-mediated toxicity (Fig. 4B). JR-159 had no effect on the DAU-mediated toxicity. In contrast, pre-incubation of NVCMs with 30 μM KH-TA4 for 6 h ($p \leq 0.01$) or with 100 μM KH-TA4 using 3 or 6 h pre-incubations significantly ($p \leq 0.01$ and $p \leq 0.0001$, respectively) increased DAU-mediated toxicity, most likely due to the toxicity observed upon incubation with KH-TA4 (100 μM) alone (Fig. 4A).

In addition to DAU, the potential cardioprotective effects of these compounds were also determined using a model of oxidative stress induced by H_2O_2 (300 μM; Fig. 4C), which induced LDH release that was comparable to that of DAU (Fig. 4B). In contrast to DAU-induced toxicity, DEX did not protect myocytes against H_2O_2-induced LDH release at any concentration or pre-incubation time (Fig. 4C). Conversely, both MK-15 and ES-5 mediated

significant cytoprotection at the highest concentrations used (100 μM) after either no preincubation (0 h, ES-5, ($p \leq 0.01$)), 6 h pre-incubation ($p \leq 0.001$ for MK-15 and $p \leq 0.0001$ for ES-5), or 24 h pre-incubation (ES-5, $p \leq 0.0001$, Fig. 4C). However, after a 3 h pre-incubation, 10 μM ES-5 significantly ($p \leq 0.05$) increased H_2O_2-induced toxicity. The analogues of ADR-925 also displayed some protection against H_2O_2-mediated LDH release. JR-159 (100 μM) was effective without a pre-incubation ($p \leq 0.05$, Fig. 4C). After a 3 h pre-incubation, significant protection was observed at all three examined concentrations (10, 30 and 100 μM) of KH-TA4 ($p \leq 0.01$, $p \leq 0.0001$ and $p \leq 0.05$, respectively), but surprisingly, none of the concentrations of JR-159 examined were effective. The most pronounced decrease in H_2O_2-mediated LDH release was observed after a 6 h pre-incubation of cardiomyocytes with 100 μM KH-TA4 (Fig. 4C). Under these conditions, protection was also observed with 30 μM KH-TA4 and 10 μM JR-159. After 24 h of pre-incubation, 100 μM JR-159 displayed significant ($p \leq 0.0001$) protection against H_2O_2-induced toxicity (Fig. 4C).

A 3 h incubation of NVCMs with DAU (1.2 μM) resulted in marked changes in cardiomyocyte morphology, including cytoplasmic vacuolization and granulation, nuclear and cellular shrinkage and detachment (Fig. 5). In addition, staining with the JC-1 probe revealed a transition from normal red-stained mitochondria with polarized inner membranes to diffuse green cytosolic fluorescence in mostly shrunken (presumably apoptotic) cells with depolarized mitochondria (Fig. 5). Pre-incubation with DEX (10 μM) partially prevented these ANT-induced changes in cellular morphology and mitochondrial inner membrane potential. This was also observed in experiments with MK-15 and ES-5 at 10 μM, while cells pre-incubated with JR-159 or KH-TA4 at 10 μM showed distinctively decreased mitochondrial function compared to DEX-pre-incubated cells (Fig. 5).

3.3 *In vivo* cardiotoxicity and cardioprotection

After 10 weeks of administration, DAU induced the premature death of 2 out of 6 animals, with both deaths occurring before the scheduled end of the treatment period (Fig. 6A). Marked heart dilation, along with significant pleural effusion and ascites were observed in both cases in a necropsy examination, which suggested the development of severe chronic ANT cardiotoxicity, as shown previously in this model.[30] Similar findings, although less pronounced were observed in the animals that survived until the end of DAU treatment. Co-treatment with DEX resulted in complete survival, and no signs of blood congestion or heart dilation were found during autopsy. On the other hand, co-treatment with KH-TA4 resulted in two premature deaths in weeks 4 and 5 (Fig. 6A). However, no signs of congestive heart failure or any other gross pathology were identified in the heart and other organs during the necropsy, suggesting that these deaths were not related to chronic ANT cardiotoxicity or the development of heart failure. Further premature deaths were observed in animals co-treated with KH-TA4 ($n = 1$), ES-5 ($n = 2$) and MK-15 ($n = 1$; Fig. 6A). The necropsy findings in these animals were similar to those observed in the DAU group. The only animal that was co-treated with JR-159 survived until the end of experiment, but an autopsy of revealed marked cardiac changes that were comparable to those found in the DAU group. Chronic DAU treatment and co-treatment with KH-TA4 and MK-15 prevented normal body weight gain, leading to a significant ($p \leq 0.05$) decrease in body weight in comparison with the control group (Fig. 6B). No significant body weight changes were observed in the animals that were co-treated with DEX and ES-5compared to the control group (Fig. 6B).

A 10 weeks of DAU treatment induced a marked reduction in LV systolic function (Fig. 6C). This was particularly true for the animals that died prematurely, which showed the most

severe changes before death (a reduction of more than 50% in LV systolic function compared to the control) accompanied by the dilation of the heart chambers, indicating severe global heart failure. In contrast, DEX co-treatment effectively prevented the decrease in the LV systolic function observed upon DAU treatment alone and was comparable to the control group. However, this was not the case upon KH-TA4 and ES-5 co-treatment, where a significant ($p \leq 0.05$) decrease in LV systolic function (similar to the DAU group) was found in the animals that survived until the end stages of the study. Together with the autopsy findings, these data confirmed that the premature deaths upon KH-TA4 and ES-5 co-treatment were associated with significant cardiotoxicity and the development of heart failure. Although a rather moderate decrease in systolic function was found with MK-15, it was not significantly different from the control group. Hence, the examination of systolic function, together with the autopsy findings, in animals surviving until the end of the study, suggests the partial protective potential of MK-15. However, the animal that died prematurely in this group also showed a reduction in systolic function (approximately 25% less than the normal values) during a cardiac examination before death. Additionally, based on the pronounced blood congestion found upon necropsy (hydrothorax 145 mL, ascites 45 mL and marked dilation of all heart chambers), heart failure was the most likely explanation of this premature death. Hence, although MK-15 showed the lowest reduction in systolic function compared to controls and lower mortality than the DAU group, its potential to prevent cardiac failure was clearly inferior relative to DEX with respect to both contractility and troponin T release. The rabbit co-treated with JR-159 in a pilot experiment also showed moderate to marked systolic dysfunction (FS = 26%), which was in contrast with the excellent cardioprotection found in the DEX group.

Plasma cTnT concentrations were markedly increased in DAU-treated animals, while DEX co-treatment resulted in values that were comparable to the control (Fig. 6D). In contrast, none of the novel analogues were able to alter the release of this cardio-specific biomarker induced by DAU administration. The animal that was co-treated with JR-159 showed a very high (0.735 μg/L) concentration of this biomarker, which also demonstrated its inability to mediate any cardioprotective effects. The 3 animals that died prematurely in middle of the experiment upon KH-TA4 co-treatment (and were subsequently not included in Fig. 6D) were found to have low to moderate levels of cTnT at the time of death (0.028, 0.033 and 0.142 μg/L), which confirmed that these deaths were not related to chronic ANT cardiotoxicity.

3.4 Interaction with Fe in solution and in H9c2 cells

The ability of DEX and the novel analogues to chelate Fe was assessed fluorometrically using the calcein assay.[53] Incubation of H9c2 cells with SIH led to a significant ($p \leq 0.0001$) increase in the fluorescence of the calcein by ~6-fold relative to the control (Fig. 7A). An increase in fluorescence was also evident following the addition of 100 μM DEX, although this increase was not as pronounced relative to SIH. Interestingly, a lag phase of approximately 1 h was observed in the chelation of Fe by DEX, which may be attributed to the hydrolysis of DEX to ADR-925 in the cytoplasm (Fig. 7A). In control H9c2 cells, an increase in calcein fluorescence was observed during the first 2 h of incubation. This observation also occurred in cells incubated with DEX or KH-TA4, but not with MK-15, ES-5 and JR-159 (Fig. 7A). After 3 h, SIH, DEX and KH-TA4 all mediated a statistically significant increase in calcein fluorescence ($p \leq 0.0001$, $p \leq 0.01$ and $p \leq 0.01$, respectively)

relative to the control. In contrast, cells incubated with MK-15, ES-5 or JR-159 resulted in a significant ($p \leq 0.01$) decrease in calcein fluorescence in comparison to the control (Fig. 7A).

We also examined the ability of the new agents to displace Fe from its complex with DAU (Fig. 7B). Our positive control, the high affinity Fe chelator, SIH,[33, 54] immediately lowered the absorbance of the DAU-Fe complex almost to the level of free DAU. The only other analogue that showed the ability to compete to displace Fe from the DAU-Fe complex was JR-159, but its effect was slow and was not as effective as SIH (Fig. 7B).

We next examined the ability of DEX and its novel analogues to induce Fe release from H9c2 cells prelabeled with ^{59}Fe-transferrin.[43, 45] As seen in Fig. 7C, neither DEX nor the novel analogues were able to mediate ^{59}Fe mobilization from H9c2 cells and were comparable to the control. In contrast, the lipophilic Fe chelator, SIH, which was used as a positive control, was able to effectively and significantly ($p \leq 0.0001$) increase ^{59}Fe release relative to the control (Fig. 7C).

3.5 Interaction of the studied compounds with TOP2

To assess the effects of DEX and the novel analogues on TOP2 isoforms, the inhibitory properties of the compounds were first determined using purified human TOP2A and supercoiled DNA in plasmid relaxation assays.[55] As observed in Fig. 8A, TOP2A relaxed the supercoiled DNA substrate as expected. In contrast to 100 μM DEX, which inhibited the

relaxation activity of TOP2A, none of the novel analogues showed any inhibitory activity towards this enzyme isoform (Fig. 8A).

Furthermore, western blotting was used to determine the protein levels of TOP2B in NVCM cells. To assess the possibility that this reflects a "band depletion effect" due to the inability of topoisomerase II complexed to DNA in our samples, that were treated with sonication to enable entrance into the gel,[56] we further treated the samples with benzonase endonuclease,[57] which did not change the results (data not shown). As seen in Fig. 8B, DEX (10 μM) induced a significant ($p \leq 0.001 - 0.01$) time-dependent decrease in TOP2B levels from 6 – 24 h. In fact, at 24 h, levels of TOP2B were decreased to approximately 20% of the control (Fig. 8B). In contrast to DEX, the incubation of NVCMs with any of the novel analogues at the same concentration (10 μM) for 24 h did not lead to any significant changes in TOP2B protein levels (Fig. 8C).

4 Discussion

Despite years of extensive research, DEX remains the only drug that has shown considerable and model-independent potential to protect against ANT-induced cardiotoxicity in both experimental studies, as well as in randomized clinical trials.[4, 28] Unfortunately, little attention has been given to defining structure-activity relationships of its cardioprotective properties. Therefore, in this study, two DEX analogues and two lipophilic analogues of its putative active metabolite, ADR-925, were synthesized and evaluated. Although DEX is used as a pure enantiomer, which is about five times more soluble in water than the racemic compound,[58] several studies showed that the cardioprotective effect of DEX is not associated with the (*S*) configuration at its chiral carbon atom (Fig. 1).[59] Therefore, achiral (ES-5) or racemic DEX and ADR-925 analogues were used in this work.

The first compound, ES-5 (Fig. 1), is a closed-ring derivative of the well-known metal chelator, DTPA.[60, 61] Analogous to DEX, ES-5 is relatively lipophilic, and, in contrast to its parent ligand, DTPA, may be membrane-permeable. Furthermore, in addition to the hydrolytic cleavage of the ethyl ester moiety, it is expected to undergo bio-activation in a manner similar to DEX, *via* the hydrolytic opening of the piperazine-2,6-dione rings, resulting in the DTPA diamide.[62] The second DEX analogue, MK-15 (Fig. 1), was designed to mimic the steric properties of DEX as closely as possible, but with terminal amides instead of the parent imide moieties. The replacement of piperazin-2,6-diones by piperazin-2-ones reduces its N-H acidity and its overall capacity to act as a hydrogen bonding acceptor.

Previously, the active metabolite of DEX, ADR-925, as well as single ring-open intermediates, did not protect NVCMs from DOX toxicity, and this effect was attributed to the limited membrane permeability of the hydrophilic metabolite to enter cardiac cells.[63] Hence, in the present study, two alkylamide analogues of ADR-925, namely JR-159 and KH-TA4 (Fig. 1), were designed to enhance lipophilicity and cell membrane permeability of the putative active metabolite.

None of the novel analogues inhibited the anti-proliferative effects of DAU, which is clearly an essential prerequisite as a cardioprotective agent. However, in contrast to DEX, which dose-dependently inhibited the proliferation of HL-60 cells when examined alone, MK-15, ES-5 and JR-159 showed only limited anti-proliferative activity when assessed alone. The anti-proliferative effect of DEX has been previously attributed to its direct inhibition of TOP2[23] and this effect was also evident in our study. Importantly, changes in the structure of DEX, such as the removal of the two oxo groups from the piperazine rings, or increasing the linker length between the rings, as observed in MK-15 and ES-5, respectively, have a marked impact on both TOP2A inhibition and the subsequent anti-proliferative activity of these analogues. Although KH-TA4 showed significant anti-proliferative activity, the effect was non-specific, as KH-TA4 also displayed toxicity towards cardiomyocytes.

DEX was able to protect NVCMs from DAU-mediated toxicity at all pre-incubation times and almost completely prevented DAU-induced morphological changes, as well as the loss of mitochondrial membrane potential. DEX also showed effective cardioprotective activity *in vivo*. However, none of the novel analogues herein provided the same degree of protection as DEX. Although MK-15 did not protect isolated cardiomyocytes from DAU, it showed weak

cardioprotective effects *in vivo* based on overall survival, LV systolic function and cTnT release. While ES-5 showed some cardioprotective effects comparable to DEX *in vitro,* its co-administration *in vivo* slightly aggravated DAU toxicity, resulting in higher overall mortality with no significant cardioprotection. The ADR-925 analogue, KH-TA4 resulted in NVCM toxicity *in vitro* at higher concentrations and did not have a significant impact on ANT cardiotoxicity *in vivo,* but instead, increased mortality due to off-target effects.

Interestingly, we also showed that DEX failed to offer any protection to cardiomyocytes exposed to the oxidative stress-inducing agent, H_2O_2 (Fig. 4). This obsevation is in contrast to the near complete protection of cells by effective Fe chelators, such as SIH, in similar experiments.[33, 64] These observations suggest DAU toxicity in cardiomyocytes is mediated by mechanism(s) that are separate from oxidative damage by H_2O_2.

Hasinoff *et al.*[63] previously showed that ADR-925 and DEX displaced Fe from its calcein complex in solution. In our study, DEX removed Fe from the calcein in H9c2 cells, but was 4-fold less efficient than the well-characterized chelator, SIH,[33, 65] and comparable results were also obtained with KH-TA4. The other analogues, MK-15, ES-5 and JR-159, instead reduced the cellular calcein fluorescence, which may be related to some interaction with calcein. Although we did not detect any intracellular chelation by ES-5 and MK-15 after 3 hours of incubation, it is possible that after longer periods (24 - 48 hours) MK-15 and ES-5 would be hydrolyzed. Indeed, this is indicated by their partial ability to protect from H_2O_2-induced toxicity. However, ES-5 and MK-15 were mostly unable to protect from DAU-induced toxicity after these longer incubation periods, which again points to the difference of H_2O_2- and DAU-induced toxicity. Cellular ^{59}Fe efflux experiments revealed that none of the

examined agents, including DEX, were able to induce Fe mobilization from H9c2 cells. However, we again cannot exclude the possibility that there was not enough time for DEX hydrolysis to occur in these experiments.

Previously, only a few bis-dioxopiperazine agents have been evaluated with respect to cardioprotective effects against chronic ANT cardiotoxicity with variable outcomes.[48, 66] Importantly, other studies have concluded that the chelation of Fe and the displacement of Fe from the ANT-Fe complex do not correlate with the cardioprotective effects of the bisdioxopiperazine derivatives.[48] This finding is in agreement with the current results and suggests factors other than Fe chelation are involved in cardioprotection. Notably, we have previously failed to find a strong association between the cardioprotective effects of DEX and the suppression of ANT-induced markers of oxidative stress in the myocardium.[31, 67] Furthermore, different biocompatible Fe chelators have been found to possess limited to no cardioprotective potential under clinically relevant conditions.[28]

Importantly, it has been noted that a number of effective DEX derivatives were catalytic inhibitors of TOP2.[66] This observation was confirmed by studies comparing the cardioprotective effects of DEX and the TOP2-inactive bis-dioxopiperazine analogue, ICRF-161.[68] Both of these compounds were hydrolyzable, comparable in displacement of Fe from its complex with DOX, but only DEX, which is an effective TOP2 inhibitor, protected spontaneously hypertensive rats from chronic ANT toxicity.[68]

There are two distinct mammalian TOP2 isoforms, TOP2A and TOP2B.[69] TOP2A is predominantly expressed in proliferating and undifferentiated cells.[70] On the contrary, TOP2B

is the major TOP2 form in resting and differentiated tissue, including the post-mitotic cardiomyocytes.[70] In the study of Lyu *et al.*,[21] using H9c2 immortalized cell line, which contains both TOP2 isoforms, DEX induced proteasome-dependent depletion of TOP2B. Data obtained in the present study using NVCMs demonstrate that DEX-induced TOP2B depletion also occurs in non-proliferating isolated cardiomyocytes. A recent study[20] reported that a conditional TOP2B knockout protected cardiomyocytes from DNA double-strand breaks and transcriptome changes induced by acute *in vivo* DOX treatment and prevented defective mitochondrial biogenesis and ROS formation. Moreover, DOX-treated TOP2B knockout mice showed no signs of progressive heart failure in the same study.[20] The results of this study indicate that Fe chelation may be not important in DEX-induced protection against DAU-induced cardiotoxicity. Hence, together with the results of above mentioned studies it might be suggested that the ability of DEX to inhibit and/or deplete TOP2B in cardiomyocytes prior to ANT exposure may be essential for effective cardioprotection, and the lack of inhibition of TOP2 activity is the plausible reason for the limited cardioprotective efficiency of the four novel DEX analogues examined in the present study. Nevertheless, we still cannot rule out the possibility that both Fe chelation (after the hydrolysis of DEX to ADR-925) and interaction with TOP2B by parent DEX are both involved in DEX-induced cardioprotection.

In conclusion, ANTs remain important components of numerous chemotherapeutic protocols, but the risk of cardiotoxicity hampers their clinical usefulness. The ability to rationally design effective cardioprotective agents depends on our understanding of the molecular basis of ANT cardiotoxicity. Data from the present study concur with the increasing body of evidence suggesting that TOP2B can be more relevant target for cardioprotection than intracellular Fe chelation. These findings contribute new structure-activity relationships of the

cardioprotective action of bisdioxopiperazine agents against ANT cardiotoxicity and will be used for further development of effective cardioprotective agents.

Funding Sources

This work was supported by the Czech Science Foundation (13-15008S), the European Social Fund and the state budget of the Czech Republic (Operational Program CZ.1.07/2.3.00/30.0022) and the Charles University in Prague (SVV 267 004, PRVOUK P37/5). D.S.K. is the recipient of a National Health and Medical Research Council of Australia (NHMRC) Project Grant (1048972), a NHMRC R.D. Wright Fellowship (1083057) and a Helen and Robert Ellis Fellowship from the Sydney Medical School Foundation of The University of Sydney. D.R.R. thanks the National Health and Medical Research Council of Australia for a Senior Principal Research Fellowship and Project Grants.

Acknowledgments

The authors thank to Mrs. Alena Pakostová and Mrs. Klára Lindrová for technical assistance.

Conflict of interest

The authors wish to acknowledge that M.T.M. is a founder, CEO and member of the Scientific Advisory Board for TopoGEN, Inc.

References

1. L. Brunton, B. Chabner and B. Knollman, *Goodman and Gilman's The Pharmacological Basis of Therapeutics, Twelfth Edition*, McGraw-Hill Professional, 2010.
2. F. Zunino and G. Capranico, *Anti-Cancer Drug Des.*, 1990, **5**, 307-317.
3. M. S. Ewer and E. T. H. Yeh, *Cancer and the Heart*, BC Decker, U.S.A., Hamilton, 2006.
4. E. C. van Dalen, H. N. Caron, H. O. Dickinson and L. C. Kremer, *Cochrane Database Syst Rev*, 2011, DOI: 10.1002/14651858.CD003917.pub4, CD003917.
5. E. C. van Dalen, H. J. van der Pal, W. E. Kok, H. N. Caron and L. C. Kremer, *Eur. J. Cancer*, 2006, **42**, 3191-3198.
6. R. Altena, P. J. Perik, D. J. van Veldhuisen, E. G. de Vries and J. A. Gietema, *Lancet Oncol.*, 2009, **10**, 391-399.
7. H. G. Keizer, H. M. Pinedo, G. J. Schuurhuis and H. Joenje, *Pharmacol. Ther.*, 1990, **47**, 219-231.
8. E. T. Yeh and C. L. Bickford, *J. Am. Coll. Cardiol.*, 2009, **53**, 2231-2247.
9. J. Goodman and P. Hochstein, *Biochem. Biophys. Res. Commun.*, 1977, **77**, 797-803.
10. T. Simunek, M. Sterba, O. Popelova, M. Adamcova, R. Hrdina and V. Gersl, *Pharmacol. Rep.*, 2009, **61**, 154-171.
11. B. Halliwell and J. Gutteridge, *Free Radicals in Biology and Medicine*, Oxford University Press, USA, 2007.
12. J. M. Fulbright, W. Huh, P. Anderson and J. Chandra, *Curr. Oncol. Rep.*, 2010, **12**, 411-419.
13. R. S. Cvetkovic and L. J. Scott, *Drugs*, 2005, **65**, 1005-1024.
14. B. B. Hasinoff, K. Hellmann, E. H. Herman and V. J. Ferrans, *Curr. Med. Chem.*, 1998, **5**, 1-28.
15. K. Kiyomiya, S. Matsuo and M. Kurebe, *Cancer Chemother. Pharmacol.*, 2001, **47**, 51-56.
16. G. Minotti, P. Menna, E. Salvatorelli, G. Cairo and L. Gianni, *Pharmacol. Rev.*, 2004, **56**, 185-229.
17. B. B. Hasinoff, *Cardiovasc. Toxicol.*, 2002, **2**, 111-118.
18. E. Ramu, A. Korach, E. Houminer, A. Schneider, A. Elami and H. Schwalb, *Cardiovasc Drugs Ther*, 2006, **20**, 343-348.

19. P. Heisig, *Mutagenesis*, 2009, **24**, 465-469.

20. S. Zhang, X. Liu, T. Bawa-Khalfe, L. S. Lu, Y. L. Lyu, L. F. Liu and E. T. Yeh, *Nat. Med.*, 2012, **18**, 1639-1642.

21. Y. L. Lyu, J. E. Kerrigan, C. P. Lin, A. M. Azarova, Y. C. Tsai, Y. Ban and L. F. Liu, *Cancer Res.*, 2007, **67**, 8839-8846.

22. J. L. Speyer, M. D. Green, A. Zeleniuch-Jacquotte, J. C. Wernz, M. Rey, J. Sanger, E. Kramer, V. Ferrans, H. Hochster, M. Meyers and et al., *J. Clin. Oncol.*, 1992, **10**, 117-127.

23. W. Rhomberg and K. Hellmann, *Razoxane and Dexrazoxane - Two Multifunctional Agents*, Springer Netherlands, Dordrecht, 1 edn., 2011.

24. H. Hochster, L. Liebes, S. Wadler, R. Oratz, J. C. Wernz, M. Meyers, M. Green, R. H. Blum and J. L. Speyer, *J. Natl. Cancer Inst.*, 1992, **84**, 1725-1730.

25. C. K. Tebbi, W. B. London, D. Friedman, D. Villaluna, P. A. De Alarcon, L. S. Constine, N. P. Mendenhall, R. Sposto, A. Chauvenet and C. L. Schwartz, *J. Clin. Oncol.*, 2007, **25**, 493-500.

26. S. M. Swain, F. S. Whaley, M. C. Gerber, S. Weisberg, M. York, D. Spicer, S. E. Jones, S. Wadler, A. Desai, C. Vogel, J. Speyer, A. Mittelman, S. Reddy, K. Pendergrass, E. Velez-Garcia, M. S. Ewer, J. R. Bianchine and R. A. Gams, *J. Clin. Oncol.*, 1997, **15**, 1318-1332.

27. U. S. F. a. D. Administration, FDA Statement on Dexrazoxane, http://www.fda.gov/Drugs/DrugSafety/ucm263729.htm, (accessed Mar 30, 2013).

28. M. Sterba, O. Popelova, A. Vavrova, E. Jirkovsky, P. Kovarikova, V. Gersl and T. Simunek, *Antioxid. Redox Signal.*, 2013, **18**, 899-929.

29. V. Gersl and R. Hrdina, *Sb. Ved. Pr. Lek. Fak. Karlovy Univerzity Hradci Kralove*, 1994, **37**, 49-55.

30. T. Simunek, I. Klimtova, J. Kaplanova, Y. Mazurova, M. Adamcova, M. Sterba, R. Hrdina and V. Gersl, *Eur. J. Heart Fail.*, 2004, **6**, 377-387.

31. O. Popelova, M. Sterba, P. Haskova, T. Simunek, M. Hroch, I. Guncova, P. Nachtigal, M. Adamcova, V. Gersl and Y. Mazurova, *Br. J. Cancer*, 2009, **101**, 792-802.

32. R. Gallagher, S. Collins, J. Trujillo, K. McCredie, M. Ahearn, S. Tsai, R. Metzgar, G. Aulakh, R. Ting, F. Ruscetti and R. Gallo, *Blood*, 1979, **54**, 713-733.

33. T. Simunek, M. Sterba, O. Popelova, H. Kaiserova, M. Adamcova, M. Hroch, P. Haskova, P. Ponka and V. Gersl, *Br. J. Pharmacol.*, 2008, **155**, 138-148.

34. S. Chlopcikova, J. Psotova and P. Miketova, *Biomed. Pap. Med. Fac. Univ. Palacky Olomouc Czech. Repub.*, 2001, **145**, 49-55.

35. W. E. Louch, K. A. Sheehan and B. M. Wolska, *J. Mol. Cell. Cardiol.*, 2011, **51**, 288-298.

36. C. Legrand, J. M. Bour, C. Jacob, J. Capiaumont, A. Martial, A. Marc, M. Wudtke, G. Kretzmer, C. Demangel, D. Duval and et al., *J. Biotechnol.*, 1992, **25**, 231-243.

37. C. Korzeniewski and D. M. Callewaert, *J. Immunol. Methods*, 1983, **64**, 313-320.

38. F. K. Chan, K. Moriwaki and M. J. De Rosa, *Methods Mol. Biol.*, 2013, **979**, 65-70.

39. B. W. Kimes and B. L. Brandt, *Exp. Cell Res.*, 1976, **98**, 367-381.

40. M. Sterba, O. Popelova, T. Simunek, Y. Mazurova, A. Potacova, M. Adamcova, H. Kaiserova, P. Ponka and V. Gersl, *J. Pharmacol. Exp. Ther.*, 2006, **319**, 1336-1347.

41. O. Popelova, M. Sterba, T. Simunek, Y. Mazurova, I. Guncova, M. Hroch, M. Adamcova and V. Gersl, *J. Pharmacol. Exp. Ther.*, 2008, **326**, 259-269.

42. H. Glickstein, R. B. El, G. Link, W. Breuer, A. M. Konijn, C. Hershko, H. Nick and Z. I. Cabantchik, *Blood*, 2006, **108**, 3195-3203.

43. D. R. Richardson, E. H. Tran and P. Ponka, *Blood*, 1995, **86**, 4295-4306.

44. D. R. Richardson and K. Milnes, *Blood*, 1997, **89**, 3025-3038.

45. E. Baker, D. Richardson, S. Gross and P. Ponka, *Hepatology*, 1992, **15**, 492-501.

46. G. Zanninelli, H. Glickstein, W. Breuer, P. Milgram, P. Brissot, R. C. Hider, A. M. Konijn, J. Libman, A. Shanzer and Z. I. Cabantchik, *Mol. Pharmacol.*, 1997, **51**, 842-852.

47. B. B. Hasinoff, D. Patel and X. Wu, *Free Radic. Biol. Med.*, 2003, **35**, 1469-1479.

48. E. H. Herman, J. Zhang, B. B. Hasinoff, D. P. Chadwick, J. R. Clark, Jr. and V. J. Ferrans, *Cancer Chemother. Pharmacol.*, 1997, **40**, 400-408.

49. A. Benjahad, R. Benhaddou, R. Granet, M. Kaouadji, P. Krausz, S. Piekarski, F. Thomasson, C. Bosgiraud and S. Delebassee, *Tetrahedron Lett.*, 1994, **35**, 9545-9548.

50. *US Pat.,* 7,381,822, 2005.

51. *Pat.,* WO 2006/051851 A1, 2006.

52. Br. *Pat.,* GB961065 (A), 1962.

53. B. P. Esposito, S. Epsztejn, W. Breuer and Z. I. Cabantchik, *Anal. Biochem.*, 2002, **304**, 1-18.

54. M. Horackova, P. Ponka and Z. Byczko, *Cardiovasc. Res.*, 2000, **47**, 529-536.

55. M. A. Bjornsti and N. Osheroff, *DNA topoisomerase protocols volume II: Enzymology and drugs*, 1999.

56. M. A. Bjornsti and N. Osheroff, *DNA topoisomerase protocols volume I: DNA topology and enzymes*, 1999.

57. E. P. Quinlivan and J. F. Gregory, 3rd, *Anal. Biochem.*, 2008, **373**, 383-385.

58. A. J. Repta, M. J. Baltezor and P. C. Bansal, *J Pharm Sci*, 1976, **65**, 238-242.

59. E. H. Herman, R. M. Mhatre and D. P. Chadwick, *Toxicol Appl Pharmacol*, 1974, **27**, 517-526.

60. F. Menetrier, L. Grappin, P. Raynaud, C. Courtay, R. Wood, S. Joussineau, V. List, G. N. Stradling, D. M. Taylor, P. Berard, M. A. Morcillo and J. Rencova, *Appl. Radiat. Isot.*, 2005, **62**, 829-846.

61. Z. N. Kazzi, A. Heyl and J. Ruprecht, *Curr. Pharm. Biotechnol.*, 2012, **13**, 1957-1963.

62. E. Graf, J. R. Mahoney, R. G. Bryant and J. W. Eaton, *J. Biol. Chem.*, 1984, **259**, 3620-3624.

63. B. B. Hasinoff, P. E. Schroeder and D. Patel, *Mol. Pharmacol.*, 2003, **64**, 670-678.

64. T. Simunek, C. Boer, R. A. Bouwman, R. Vlasblom, A. M. Versteilen, M. Sterba, V. Gersl, R. Hrdina, P. Ponka, J. J. de Lange, W. J. Paulus and R. J. Musters, *J. Mol. Cell. Cardiol.*, 2005, **39**, 345-354.

65. P. Ponka, J. Borova, J. Neuwirt and O. Fuchs, *FEBS Lett.*, 1979, **97**, 317-321.

66. E. H. Herman, A. N. el-Hage, A. M. Creighton, D. T. Witiak and V. J. Ferrans, *Res. Commun. Chem. Pathol. Pharmacol.*, 1985, **48**, 39-55.

67. E. Jirkovsky, O. Popelova, P. Krivakova-Stankova, A. Vavrova, M. Hroch, P. Haskova, E. Brcakova-Dolezelova, S. Micuda, M. Adamcova, T. Simunek, Z. Cervinkova, V. Gersl and M. Sterba, *J. Pharmacol. Exp. Ther.*, 2012, **343**, 468-478.

68. E. Martin, A. V. Thougaard, M. Grauslund, P. B. Jensen, F. Bjorkling, B. B. Hasinoff, J. Tjornelund, M. Sehested and L. H. Jensen, *Toxicology*, 2009, **255**, 72-79.

69. F. H. Drake, J. P. Zimmerman, F. L. McCabe, H. F. Bartus, S. R. Per, D. M. Sullivan, W. E. Ross, M. R. Mattern, R. K. Johnson, S. T. Crooke and et al., *J. Biol. Chem.*, 1987, **262**, 16739-16747.

70. G. Capranico, S. Tinelli, C. A. Austin, M. L. Fisher and F. Zunino, *Biochim. Biophys. Acta*, 1992, **1132**, 43-48.

Figure 1

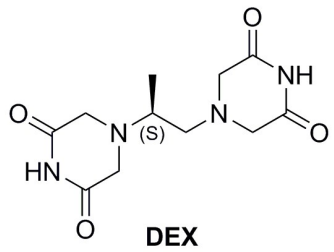

DEX

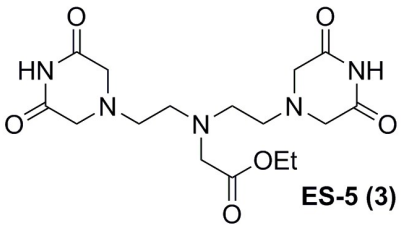

ES-5 (3)

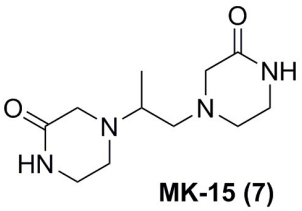

MK-15 (7)

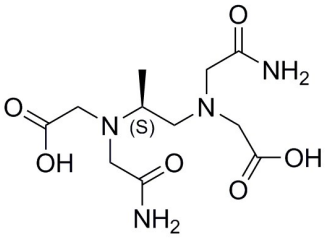

ADR-925

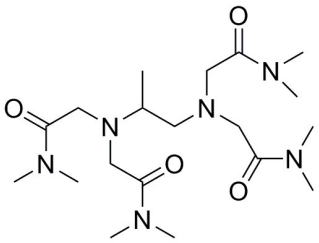

JR-159 (10)

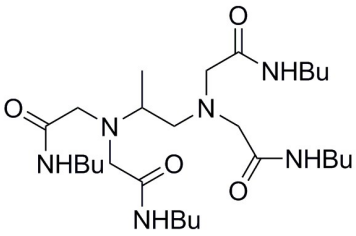

KH-TA4 (12)

Figure 2

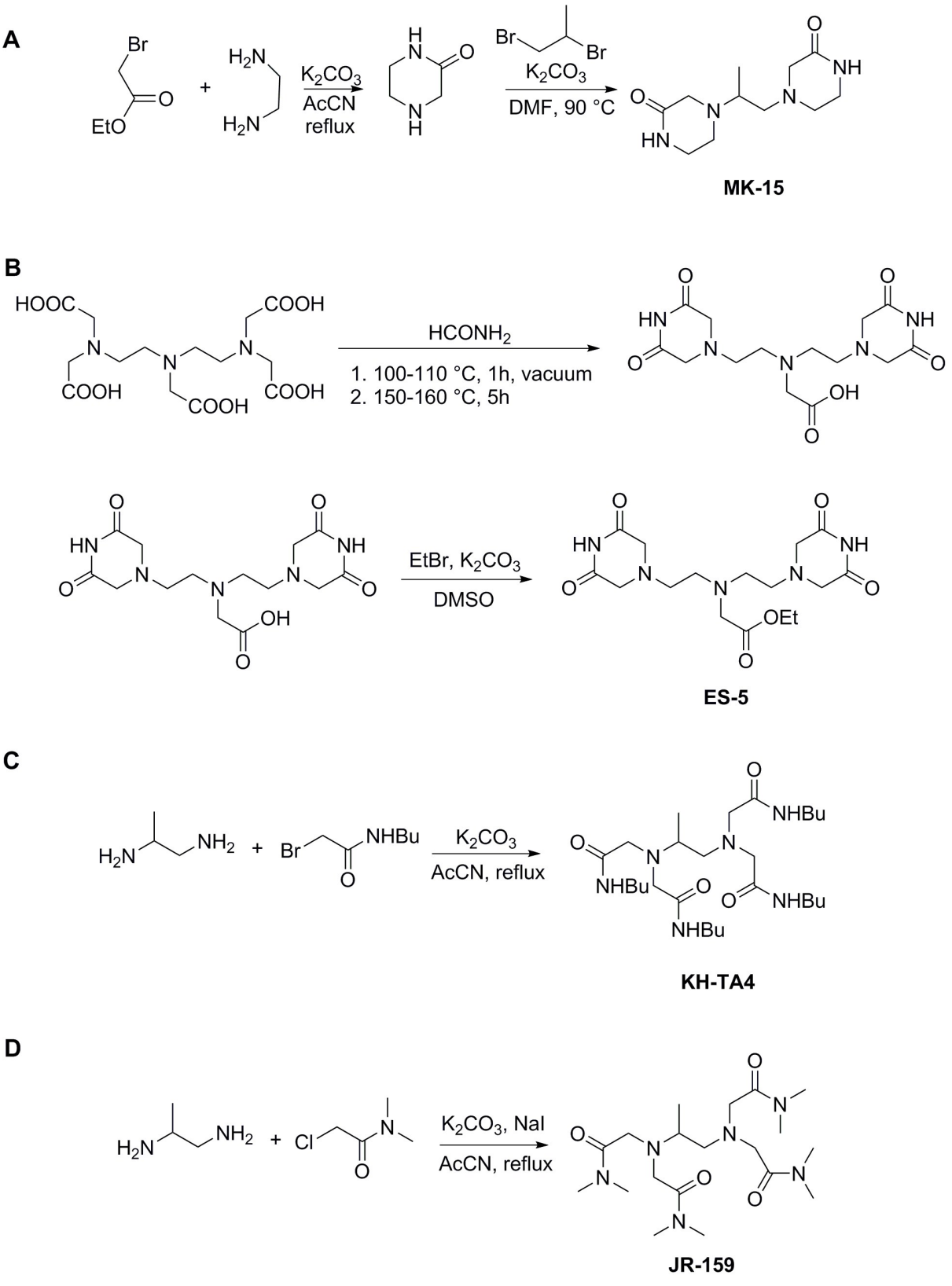

Figure 3

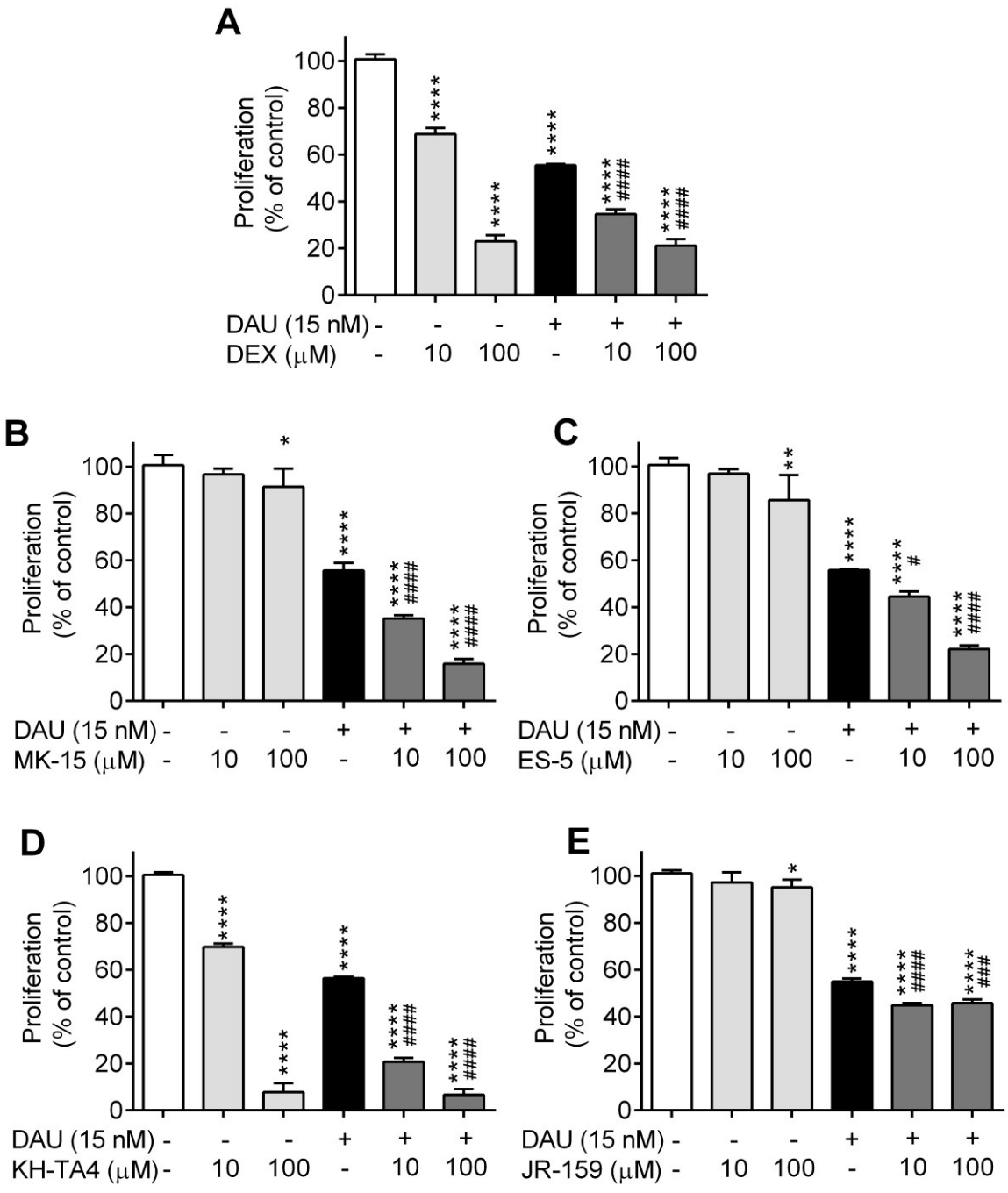

Figure 4

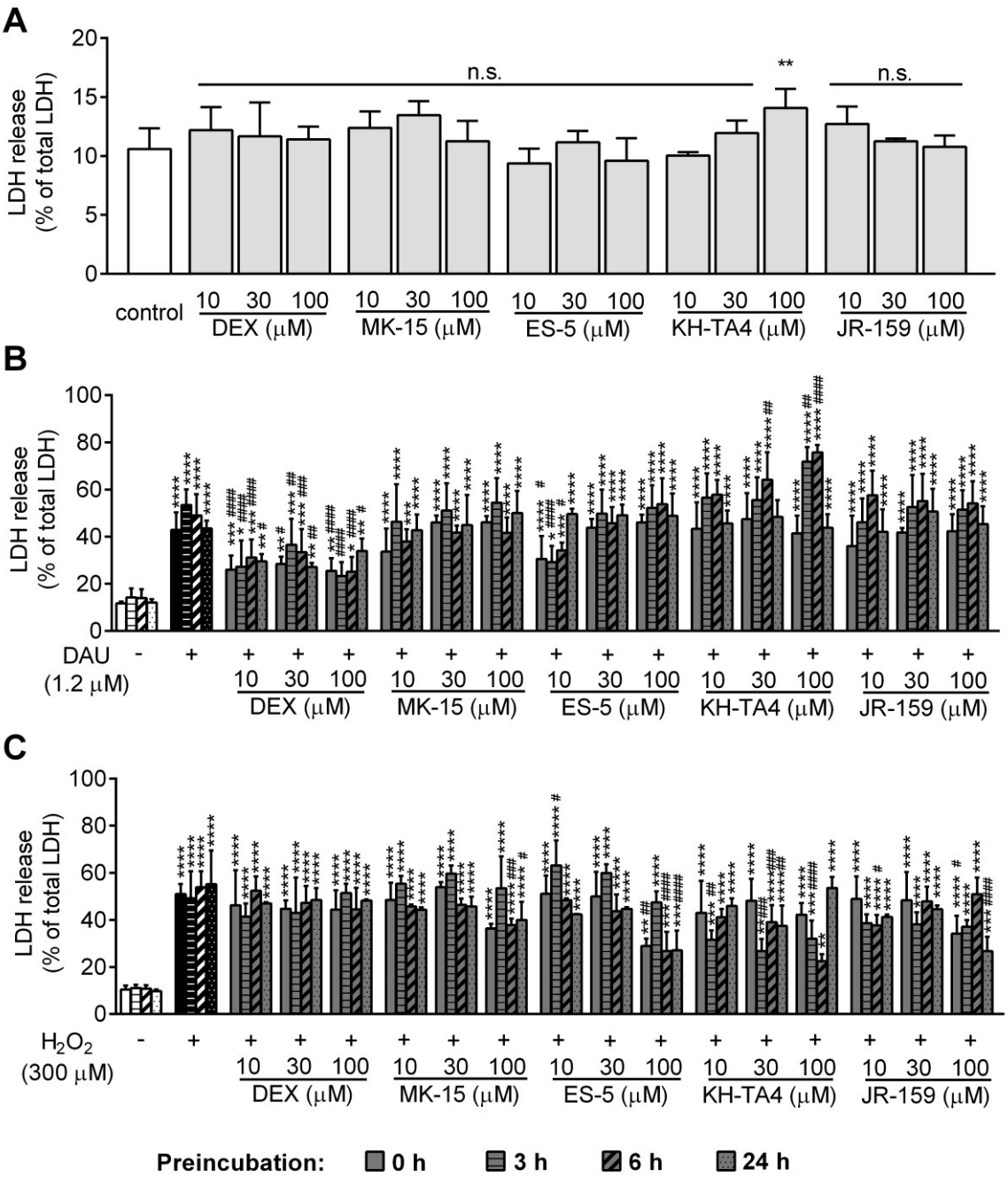

Figure 5

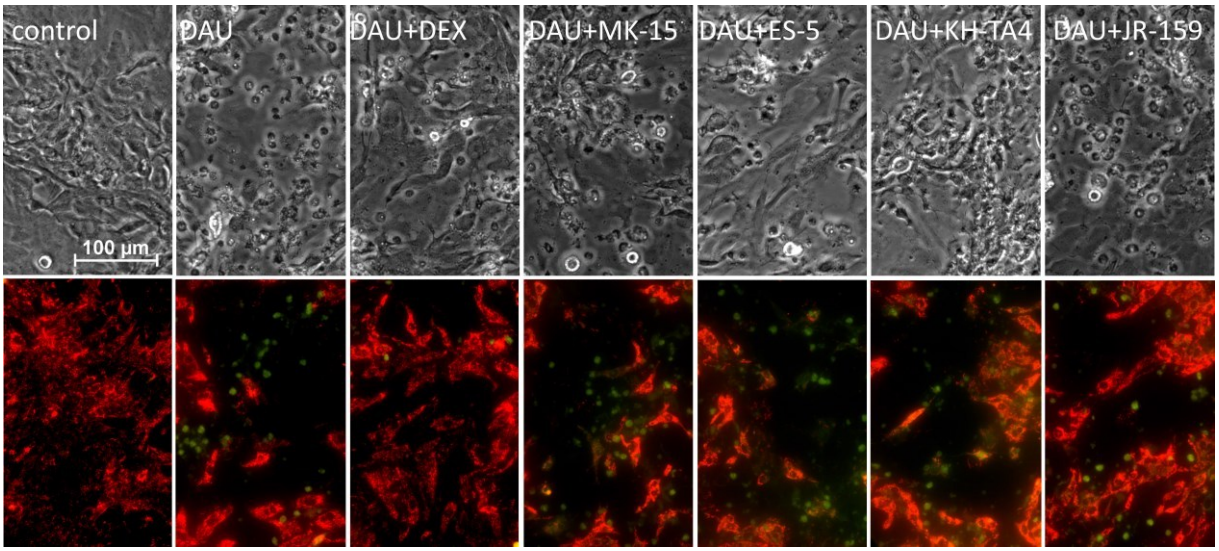

Figure 6

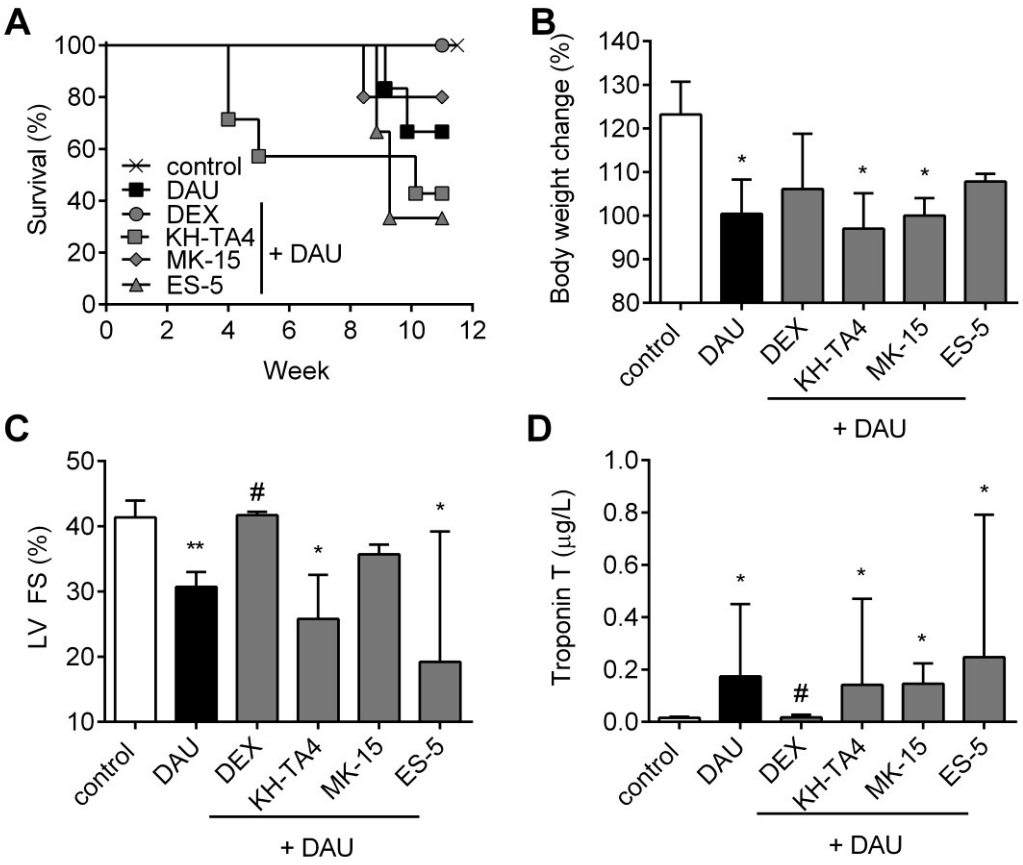

Figure 7

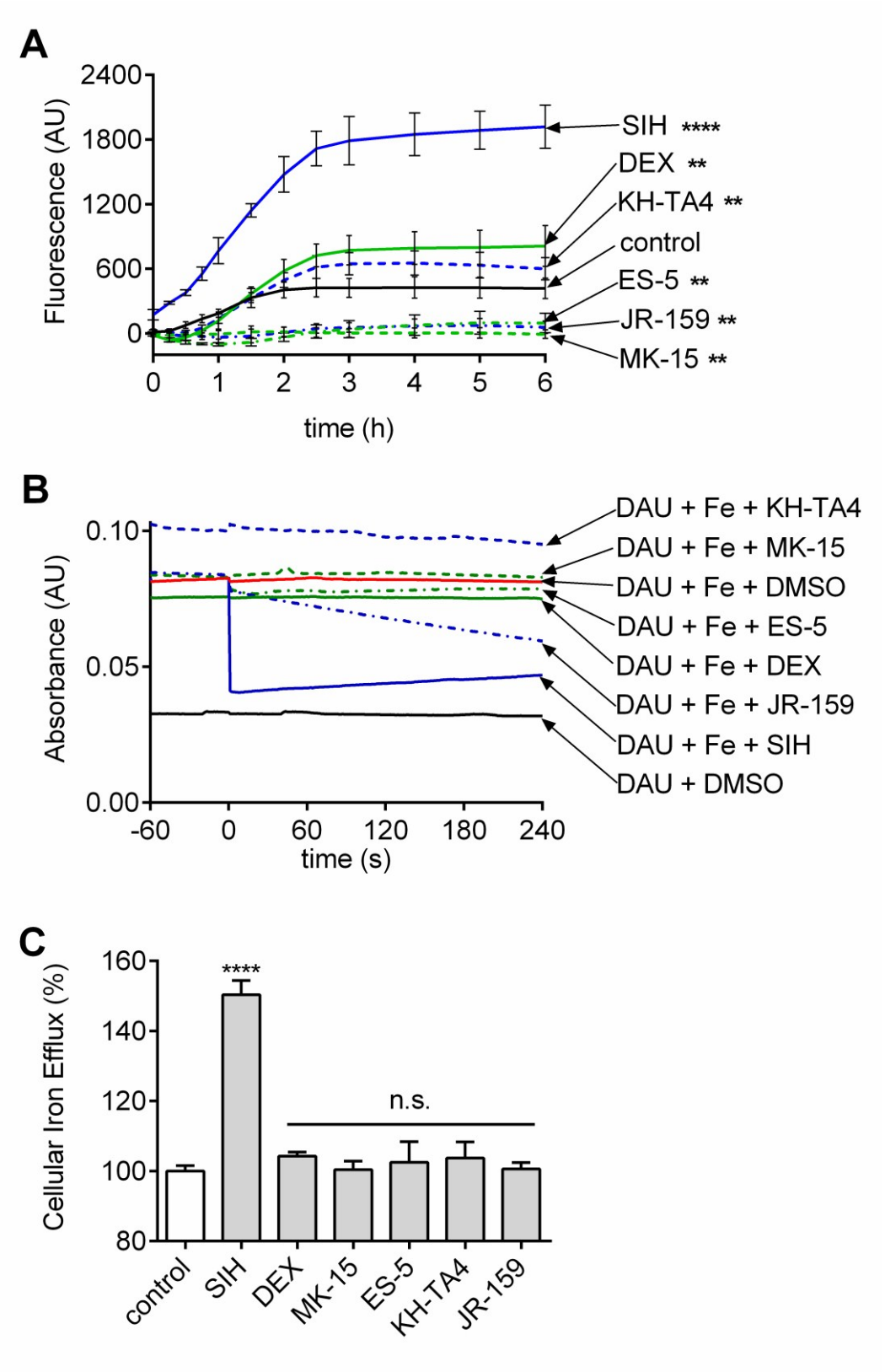

Figure 8

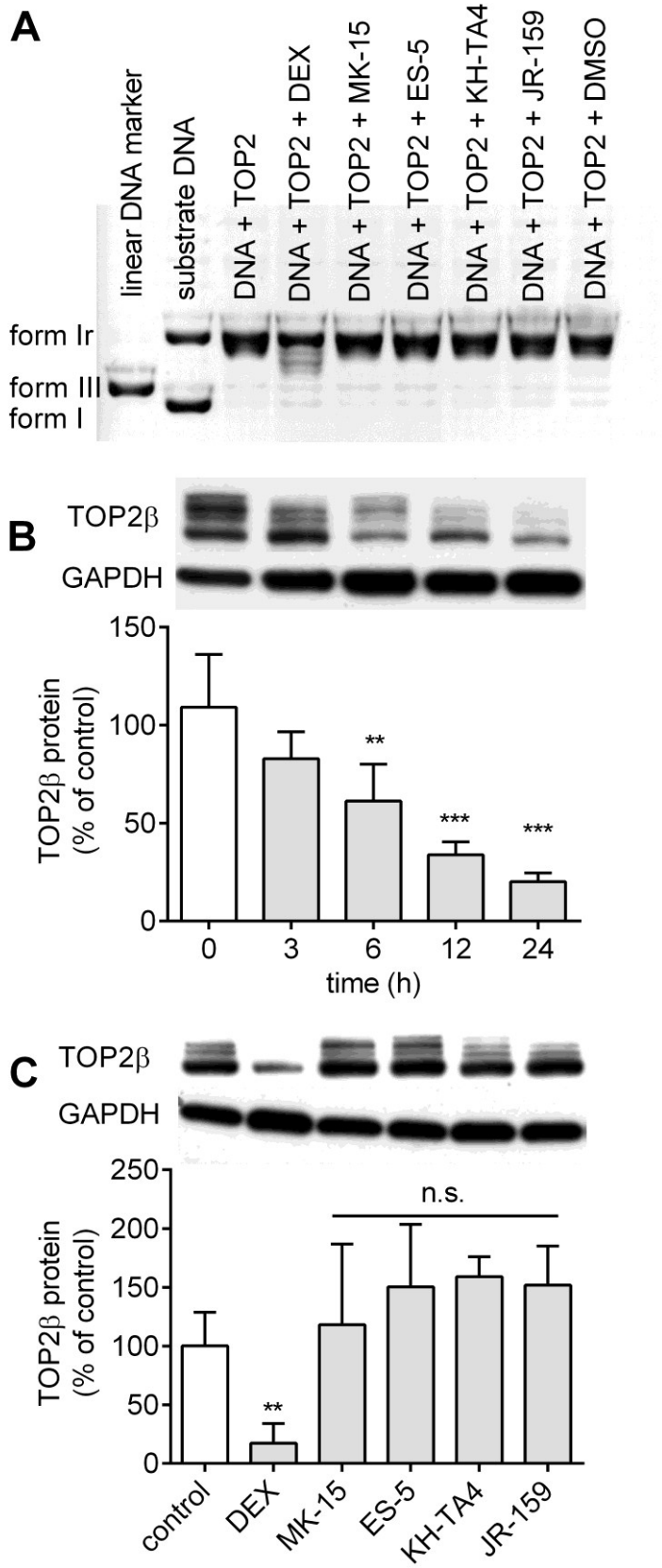

Figure legends

Figure 1. Chemical structures of dexrazoxane (DEX), its putatively active metabolite, ADR-925, and the four newly synthesized analogues examined in this study, MK-15, ES-5, KH-TA4 and JR-159.

Figure 2. Syntheses of the new analogues of dexrazoxane (DEX) and its metabolite ADR-925: 4,4'-(Propane-1,2-diyl)bis(piperazin-2-one) (**MK-15; A**); Ethyl-2-{bis[2-(3,5-dioxopiperazin-1-yl)ethyl]amino}acetate (**ES-5; B**); *N,N,N′,N′*-tetrakis(*N*-butylcarbamoylmethyl)-1,2-diaminopropane (**KH-TA4; C**); *N,N,N′,N′*-tetrakis(*N,N*-dimethylcarbamoylmethyl)-1,2-diaminopropane **10** (**JR-159; D**).

Figure 3. Anti-proliferative activity of dexrazoxane (DEX), MK-15, ES-5, KH-TA4 and JR-159 alone and in combination with daunorubicin (DAU). HL-60 cells were incubated with 10 or 100 μM DEX (A), MK-15 (B), ES-5 (C), KH-TA4 (D), and JR-159 (E) alone or in combination with 15 nM DAU for 72 h/37ºC. The viability of the cells was assessed using MTT assays. The data are presented as the mean ± SD of four independent experiments. Statistical significance was evaluated using one-way ANOVA and Holm-Sidak's post-hoc test; *–compared to control, #–compared to DAU (****/#### $p \leq 0.0001$, ***/### $p \leq 0.001$, **/## $p \leq 0.01$, */# $p \leq 0.05$).

Figure 4. Toxicities of dexrazoxane (DEX), MK-15, ES-5, KH-TA4 and JR-159 and their effects on daunorubicin (DAU)- and hydrogen peroxide (H_2O_2)-induced toxicity in neonatal ventricular rat cardiomyocytes (NVCM cells). NVCM cells were incubated with DEX, MK-15, ES-5, KH-TA4 and JR-159 for 48 h (A), or pre-incubated with these substances for 0, 3, 6 and 24 h and then incubated with either DAU for 3 h following a 48 h DAU-free period (B) or H_2O_2 for 48 h (C). The toxicity was assessed by measuring the release of lactate dehydrogenase (LDH) into the culture medium. These data are presented as the mean ± SD of more than three independent experiments. Statistical significance was evaluated using one-way ANOVA and Holm-Sidak's post-hoc test; * – compared to control, # – compared to DAU/H_2O_2 DAU (****/#### $p \leq 0.0001$, ***/### $p \leq 0.001$, **/## $p \leq 0.01$, */# $p \leq 0.05$).

Figure 5. Evaluation of cellular morphology and changes in the mitochondrial membrane potential. Neonatal ventricular cardiomyocytes were pre-treated with 30 µM dexrazoxane (DEX), MK-15, ES-5,KH-TA4 or JR-159 for 3 h, then incubated with 1.2 µM daunorubicin (DAU) for 3 h and then without drugs for 48 h. The upper panels are bright-field phase contrast photomicrographs, and the lower panels are darkfield epifluorescence images of the same cells taken after loading with the JC-1 probe. Red emission reflects the mitochondrial inner membrane potential-dependent accumulation of probe dimers in actively respiring mitochondria, and green fluorescence indicates monomers of the probe released into the cytoplasm after mitochondrial depolarization. A lack of fluorescence reflects the release of the probe from necrotic or late-stage apoptotic cells. The scale bars represent 100 µm. All photomicrographs were taken at the same magnification.

Figure 6. *In vivo* cardiotoxicity assessments. General toxicity was determined as animal survival (A) or body weight change (B). Cardiac function was assessed by measuring left ventricular fraction shortening (LV FS; C) using echocardiography. The concentration of cardiac troponin T in the plasma (D) was measured at the end of the treatment period (see *Materials and Methods*). The data are expressed as the per cent of initial values and presented as the median ± interquartile range. Statistical significance was evaluated using one-way ANOVA and Dunn's post-hoc test; * – compared to control, # – compared to DAU (**/## $p \leq 0.01$, */# $p \leq 0.05$).

Figure 7. Iron (Fe) chelation properties measured as the rate of Fe displacement from the Fe-calcein complex in H9c2 cells (A), Fe displacement from the DAU-Fe complex (B), and ^{59}Fe mobilization from H9c2 cells (C). The change of fluorescence of trapped intracellular calcein in H9c2 cells loaded with 100 μM ferric-ammonium citrate (A) was assessed after adding the Fe chelator salicylaldehyde isonicotinoyl hydrazone (SIH) as a positive control, dexrazoxane (DEX), or the novel analogues MK-15, ES-5, KH-TA4 and JR-159, all at 100 μM. The ability of the studied substances to remove Fe from its complex with DAU (B) was evaluated in time in a buffered solution after the addition of DMSO as a solvent control, SIH or other studied substances. The rate of iron mobilization from the cells induced by the studied substances (C) was measured after loading the cells with ^{59}Fe-transferrin. The representative of three measurements (B) or mean ± SD (A, C) of three independent measurements is presented. Statistical significance for panels A (after 3-hour interval of incubation) and C was evaluated using one-way ANOVA and Holm-Sidak's post-hoc test; * – compared to control (**** $p \leq 0.0001$, *** $p \leq 0.001$, ** $p \leq 0.01$, * $p \leq 0.05$), n.s. – non-significant.

Figure 8. The effects of the examined agents, dexrazoxane (DEX), MK-15, ES-5, KH-TA4 and JR-159 on the activity of topoisomerase IIα (TOP2A) (A) and the protein levels of topoisomerase IIβ (TOP2B) in neonatal rat ventricular cardiomyocytes (B, C). The influence of the studied agents on TOP2A activity (A) was measured using enzymatic assays with recombinant human TOP2A and supercoiled DNA as a substrate (Form I – supercoiled DNA, Form Ir – relaxed DNA, Form III – linear DNA). A representative result from three independent measurements is presented. Western blot analysis of the levels of TOP2B protein in NVCM cells incubated with 10 μM DEX for 0, 3, 6, 12 and 24 h/37 °C (B) or with 10 μM DEX, MK-15, ES-5, KH-TA4 and JR-159 for 24 h/37 ºC (C) assessed as described in the Materials and Methods section. The data from three independent experiments are presented as the mean ± SD. Statistical significance was evaluated using one-way ANOVA and Holm-Sidak's post-hoc test; * – compared to control (**** $p \leq 0.0001$, *** $p \leq 0.001$, ** $p \leq 0.01$, * $p \leq 0{,}05$), n.s. – non-significant.